

---

LINEARIZATION OF FM-CW RADAR  
SWEEP BY FEEDBACK

Steven Alfred Marshall

DUBLIN COUNTY LIBRARY  
NATIONAL STATE SCHOOLS  
MIDDLE Y. SCHOOL IA 93940

# NAVAL POSTGRADUATE SCHOOL

Monterey, California



## THESIS

LINEARIZATION OF FM-CW RADAR  
SWEEP BY FEEDBACK

by

Steven Alfred Marshall

December 1974

Thesis Advisor:

D.B. Hoisington

Approved for public release; distribution unlimited.

T165956



REPORT DOCUMENTATION PAGE		READ INSTRUCTIONS BEFORE COMPLETING FORM
1. REPORT NUMBER	2. GOVT ACCESSION NO.	3. RECIPIENT'S CATALOG NUMBER
4. TITLE (and Subtitle)  Linearization of FM-CW Radar Sweep by Feedback		5. TYPE OF REPORT & PERIOD COVERED Master's Thesis; December 1974
		6. PERFORMING ORG. REPORT NUMBER
7. AUTHOR(s)  Steven Alfred Marshall		8. CONTRACT OR GRANT NUMBER(s)
9. PERFORMING ORGANIZATION NAME AND ADDRESS Naval Postgraduate School Monterey, Ca. 93940		10. PROGRAM ELEMENT, PROJECT, TASK AREA & WORK UNIT NUMBERS
11. CONTROLLING OFFICE NAME AND ADDRESS Naval Postgraduate School Monterey, Ca. 93940		12. REPORT DATE December 1974
		13. NUMBER OF PAGES 88
14. MONITORING AGENCY NAME & ADDRESS (if different from Controlling Office) Naval Postgraduate School Monterey, Ca. 93940		15. SECURITY CLASS. (of this report) Unclassified
		15a. DECLASSIFICATION/DOWNGRADING SCHEDULE
16. DISTRIBUTION STATEMENT (of this Report)  Approved for public release; distribution unlimited.		
17. DISTRIBUTION STATEMENT (of the abstract entered in Block 20, if different from Report)		
18. SUPPLEMENTARY NOTES		
19. KEY WORDS (Continue on reverse side if necessary and identify by block number)  Radar FM-CW Radar Frequency Modulation Linearization		
20. ABSTRACT (Continue on reverse side if necessary and identify by block number)  A frequency-modulated radar is a radar in which a continuous-wave transmission is frequency modulated in a known manner in order to obtain range information. When the frequency modulation is linear with time, the difference between the frequency of the received signal and the transmitted signal is directly proportional to the target range. The difference frequency is given by $(2R/c)(df/dt)$ , $R$ being the range to the		



## (20. ABSTRACT continued)

target,  $c$  the velocity of electromagnetic waves and  $df/dt$  the slope of the sawtooth frequency modulation. Therefore, the difference frequency is proportional to both range and the slope of the modulated waveform. In an ideal sawtooth frequency-modulated waveform, the slope would be a constant; however, the device to be used in the portable FM-CW radar, a varactor-tuned Gunn oscillator, exhibits a non-linear frequency sweep. If the frequency sweep is non-linear, the return from a target at fixed range is frequency modulated. As a result the bandwidth of the echo signal is increased, and range resolution is impaired. Work on this thesis will be directed towards linearization of this FM sweep and, accordingly, to optimize range resolution.







Linearization of FM-CW Radar  
Sweep by Feedback

by

Steven Alfred Marshall  
Lieutenant, United States Navy  
B.S.E.E., University of Colorado, 1969

Submitted in partial fulfillment of the  
requirements for the degree of

MASTER OF SCIENCE IN ELECTRICAL ENGINEERING

from the

NAVAL POSTGRADUATE SCHOOL  
December 1974

Thesis  
M3559  
c. 1

LUTHER V. HUBBARD  
RESEARCH HUBB  
Y. HUBBARD

## ABSTRACT

A frequency-modulated radar is a radar in which a continuous-wave transmission is frequency modulated in a known manner in order to obtain range information. When the frequency modulation is linear with time, the difference between the frequency of the received signal and the transmitted signal is directly proportional to the target range. The difference frequency is given by  $(2R/c)(df/dt)$ ,  $R$  being the range to the target,  $c$  the velocity of electromagnetic waves and  $df/dt$  the slope of the sawtooth frequency modulation. Therefore, the difference frequency is proportional to both range and the slope of the modulated waveform. In an ideal sawtooth frequency-modulated waveform, the slope would be a constant; however, the device to be used in the portable FM-CW radar, a varactor-tuned Gunn oscillator, exhibits a non-linear frequency sweep. If the frequency sweep is non-linear, the return from a target at fixed range is frequency modulated. As a result the bandwidth of the echo signal is increased, and range resolution is impaired. Work on this thesis will be directed towards linearization of this FM sweep and, accordingly, to optimize range resolution.



## TABLE OF CONTENTS

I.	FREQUENCY-MODULATED RADAR -----	10
	A. FREQUENCY-MODULATED VERSUS PULSE RADAR --	10
	B. FM-CW MARINE RADAR APPLICATIONS -----	11
	C. RF SOURCE FOR FM-CW -----	13
	1. FM Generation -----	13
	2. Improving Sweep Linearity -----	13
II.	GUNN-DIODE VOLTAGE-TUNABLE OSCILLATOR -----	14
	A. CONCEPT OF LOW-POWER PORTABLE RADARS ----	14
	B. GUNN-DIODE VOLTAGE-TUNABLE OSCILLATOR CHARACTERISTICS -----	14
III.	MODULATION LINEARIZATION BY FEEDBACK -----	17
IV.	DELAY -----	19
	A. TWO METHODS FOR CREATING DELAY -----	19
	1. Delay Using Coaxial Cable -----	19
	2. Delay Using MAD Line -----	21
V.	SYSTEM PARAMETERS -----	24
	A. MODULATION FREQUENCY AND PERIOD -----	25
	B. STATIONARY TARGET AND RANGE AMBIGUITY -----	26
	C. DOPPLER FREQUENCY SHIFT AND RESULTING RANGE ERROR -----	29
	D. RANGE RESOLUTION -----	34
	E. BEAT FREQUENCY DEPENDENCE ON FREQUENCY- SWEEP BANDWIDTH -----	35
VI.	DETERMINING LINEARITY -----	40
	A. TUNED CAVITY AND PROBE METHOD -----	40
	1. Cavity Linearity -----	41
	2. Probe/Diode Detector Linearity -----	42



3.	Limitations on Cavity Use -----	45
B.	BEAT-FREQUENCY METHOD -----	48
1.	Equipment Setup -----	48
2.	Measuring Time Between Beat- Frequency Peaks -----	48
3.	Accuracy in Time Measurements -----	51
4.	Meaning of Time Measurements -----	51
VII.	FINAL EQUIPMENT SETUP -----	52
VIII.	EFFECT OF NOISE IN CORRECTION CIRCUIT -----	58
IX.	PHASE-LOCKED LOOP -----	60
X.	DELAY AND FILTERING -----	64
XI.	VOLTAGE RAMP RETRACE TIME -----	65
XII.	OPTIMUM CORRECTING VOLTAGE -----	66
XIII.	LINEARITY ANALYSIS -----	70
XIV.	OTHER METHODS OF FM LINEARIZATION -----	74
A.	SAMPLE AND HOLD METHOD -----	74
B.	ANALOG/DIGITAL METHOD -----	75
XV.	CONCLUSION -----	86
	LIST OF REFERENCES -----	87
	INITIAL DISTRIBUTION LIST -----	88





## LIST OF FIGURES

1.	Varactor-tuned Gunn oscillator change in output frequency $\Delta f$ versus varactor voltage -----	16
2.	Block diagram of basic feedback system -----	18
3.	Microwave acoustic delay device with isolators attached to input and output ports -----	23
4.	Shape of frequency swept waveform -----	24
5.	Transmitted and received signals from a stationery target at less than maximum range with resulting beat frequency shown below -----	27
6.	Transmitted and received signals from a stationary target at maximum range with resulting beat frequency shown below -----	28
7.	Transmitted and received signals from a stationary target at greater than maximum range with resulting beat frequency shown below -----	30
8.	Transmitted and received signals from a stationary target and a moving closing target at the same range showing difference in beat frequency -----	31
9.	Cavity and probe apparatus -----	42
10.	Resonant peak showing $f_0$ and $\Delta f$ -----	43
11.	Diode-detector output voltage versus varactor voltage -----	44
12.	Diode-detector output voltage versus diode-detector input voltage -----	46
13.	Power output versus varactor voltage -----	47
14.	Block diagram of equipment setup used for measuring time between peaks of the beat-frequency signal -----	49
15.	Method used for measuring time between beat frequency peaks -----	50
16.	Block diagram of final equipment setup -----	53



17.	Photograph, laboratory system assembly showing delay device, mixer, cavity and probe and circuitry view no. 1 -----	54
18.	Photograph, same as Figure 17 except view no. 2 -----	54
19.	Correcting circuit, closeup view -----	55
20.	External amplifier, closeup view -----	56
21.	Schematic diagram of correcting circuitry -----	57
22.	Block diagram of phase-locked loop -----	61
23.	Correcting signal (AC) -----	63
24.	Corrected ramp (AC) shown with correcting signal (AC) for one cycle -----	67
25.	Corrected ramp (AC) shown with correcting signal (AC) for two cycles -----	67
26.	Uncorrected output frequency waveform as obtained from cavity and probe -----	68
27.	Corrected output frequency waveform as obtained from cavity and probe -----	68
28.	Beat frequency (uncorrected) as recorded at input to PLL -----	71
29.	Beat frequency (corrected) as recorded at input to PLL -----	71
30.	Deviation of ramp slope, $df/dt$ , from average -----	73
31.	Sample and hold method No. 1 block diagram -----	76
32.	Sample and hold method No. 1 circuit waveforms (Part I) -----	77
33.	Sample and hold method No. 1 circuit waveforms (Part II) -----	78
34.	Sample and hold method No. 2 block diagram -----	79
35.	Sample and hold method No. 2 circuit waveforms --	80
36.	Block diagram of analog/digital linearization method -----	82
37.	Analog to digital error conversion -----	83



## ACKNOWLEDGEMENTS

The author wishes to thank Professor David B. Hoisington for his help and encouragement throughout the course of this thesis. Appreciation is expressed to Mr. Ernie Kirchner and to Teledyne MEC for the generous loan of a microwave acoustic delay line, without which this thesis would not have been possible. A great deal of thanks goes to Lieutenant Glenn Ewing whose helpful suggestions aided in the successful completion of this thesis. And most importantly, a million thanks to my wife, Linda, and my children for their patience and understanding during the last hectic weeks of this thesis.





## I. FREQUENCY-MODULATED RADAR

A frequency-modulated radar is a radar in which a continuous-wave transmission is frequency modulated in a known manner in order to obtain range information. The range information is obtained by comparing the received signal with the transmitted signal such that a difference frequency is obtained. This difference frequency is directly proportional to the distance to the reflecting object that caused the echo.

### A. FREQUENCY-MODULATED VERSUS PULSE RADAR

In contrast, pulse radars send out a series of short bursts or pulses of radio-frequency energy and receive the delayed echos in the silent intervals between transmitted pulses.

Since frequency-modulated radar both transmits and receives signals simultaneously, this prevents the time-division antenna duplexing used in pulse radar. Typically separate transmitting and receiving antennas are utilized when the transmitted power exceeds about one watt.

One of the advantages of FM-CW radar is that ranges of only a few feet may be measured. This explains the development of frequency-modulated radar for the measurement of altitude of aircraft. In World War II, all major combatants utilized frequency-modulated altimeters [1].



Frequency-modulated and pulse radar systems having the same average power, frequency of operation, antenna gain, signal bandwidth, signal integration times, and so on, have maximum ranges of the same order of magnitude. One advantage of FM-CW over pulse radar is that it is not required to handle the large peak power levels associated with pulse radars.

Range resolution is dependent upon the radio-frequency bandwidth (range resolution is discussed in detail in Section V). In frequency-modulated radar range resolution can be increased simply by increasing the modulation bandwidth. In conventional pulse radar increasing range resolution is accomplished by making the transmitted pulse narrower. This means that in order to obtain a given average power out of the radar, the peak power must be increased, and the system must be capable of handling the higher peak power level. Moreover, receiver bandwidth must be changed when the pulse width is changed or maximum range capability suffers. Therefore, high range resolution is more easily attained in a frequency-modulated radar, but the theoretical range resolution can only be achieved if there is a high degree of modulation linearity. The linearity must be present over the entire range of the frequency sweep.

## B. FM-CW MARINE RADAR APPLICATIONS

Frequency-modulated marine radars are designed principally for obtaining range information. These radars



would be at a great disadvantage when compared to pulse radars for application against high-speed targets. The greater the relative velocity between the radar platform and the target, the greater the doppler shift of the reflected signal; therefore, the difference frequency would be altered by this doppler shift, causing a range error. The effect of doppler-frequency shift caused by a moving target is discussed further in Section V. The pulse radar, unlike the frequency-modulated radar, does not depend upon a frequency shift to provide range information, but rather it depends only upon the time it takes for a narrow pulse of RF energy to travel from the radar, strike the target, and return to the radar. The total time of travel is directly proportional to the range to the target and is totally independent of the doppler frequency shift.

The doppler shift is not utilized in the standard pulse radar; however, there are certain pulse radars which do make use of the doppler shift to detect moving targets in clutter. These radars are known as MTI (Moving Target Indication) radars when the duty cycle is low, or pulse-doppler radars when the duty cycle is high.

The FM-CW radar can be very effective in providing accurate range information on stationary targets or targets moving with a low relative velocity where the doppler shift encountered is small, see Section V for doppler calculations.



## C. RF SOURCE FOR FM-CW

The portable FM-CW radar being designed will utilize a varactor-tuned Gunn oscillator as an RF source for reasons of practicality. The device is practical for portable applications since it is capable of operating from low voltage (typically 10 VDC) supplies and is easily frequency-modulated.

### 1. FM Generation

The frequency modulation will be generated by placing a ramp voltage on the varactor portion of a varactor-tuned Gunn oscillator. To optimize range resolution, it is necessary to obtain as linear a frequency sweep as possible. This is a problem when utilizing the Gunn diode source, as the frequency sweep obtained by placing a linear ramp voltage on the varactor is inherently non-linear over its entire range. The degree of non-linearity is small when frequency sweep is restricted to a small bandwidth, but the non-linearity increases as the sweep amplitude increases. This effect can be seen on the change in output frequency versus varactor voltage (time) curve, Figure 1.

### 2. Improving Sweep Linearity

As one possible method of improving the sweep linearity, a feedback circuit, utilizing an acoustic delay device, a microwave mixer, and a phase-locked loop as major components was used to create a correcting signal. The correcting signal was applied to the varactor in addition to the linear-voltage ramp. The combination of the two signals greatly reduced the non-linearity in the sweep.





## II. GUNN-DIODE VOLTAGE-TUNABLE OSCILLATOR

### A. CONCEPT OF LOW-POWER PORTABLE RADARS

The concept of low-power portable radars operating from low-voltage battery supplies became more appropriate with the advent of the Gunn-diode oscillator. The low-voltage supply used with the Gunn oscillators, typically 10 VDC, is less expensive and more practical than the high-voltage supply necessary for magnetron or klystron operation. Gunn oscillator development has reached the point of obtaining from approximately 5 watts continuous-wave power output at C band, to 0.5 watts continuous-wave power output at X band [2].

Police hand-held doppler radars utilizing stable CW Gunn oscillators as RF sources are capable of detecting doppler frequency shifts and converting these shifts into corresponding relative vehicle speeds. These simple doppler radars are capable of very accurate speed measurement, but they do not have range finding capabilities. By frequency modulating the CW signal, range information can be extracted from comparison of the instantaneous frequencies of transmitted and echo signals.

### B. GUNN-DIODE VOLTAGE-TUNABLE OSCILLATOR CHARACTERISTICS

The typical Gunn-diode voltage-tunable oscillator consists of a Gunn-diode oscillator with an integral varactor



diode. In the 9 GHz frequency range the apparatus typically is mechanically tunable over a bandwidth of 1-2 GHz, and voltage tunable over a wide range, typically 100 MHz, with a tuning voltage of 0-35 VDC. Figure 1 is a curve showing variation with varactor voltage for the device used in this work.

The varactor tuning provides an ideal method for generating an FM sweep since sweeping the dc voltage on the varactor causes a frequency shift proportional to the amount of voltage applied. This frequency modulation of the RF signal provides the necessary reference point to obtain range information.

The varactor-tuned Gunn oscillator is extremely sturdy. With a little caution exercised when applying maximum bias conditions, the device should give many thousands of maintenance-free hours of operation. Solid-state sources have life expectancies in excess of 100,000 hours, but with the attached varactor, mean life time between failure varies between 2000 hours and 40,000 hours of operation for the varactor-tuned Gunn oscillator [3].

The long lifetime along with the low-voltage supply used with the Gunn oscillator makes it possible to design a low-power FM-CW radar that is small in size and weight while requiring a minimum of maintenance.



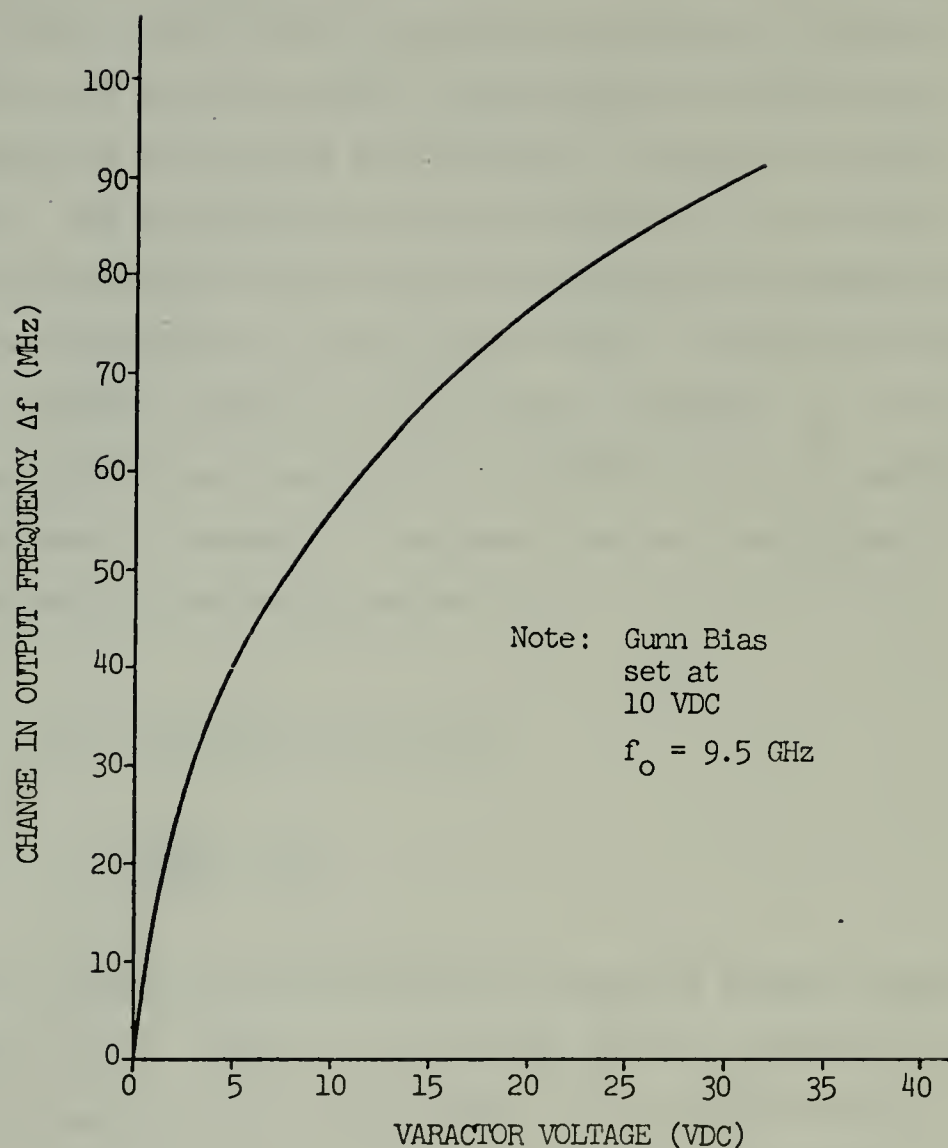


FIGURE 1. Varactor tuned Gunn Oscillator  
change in output frequency  $\Delta f$   
versus varactor voltage





### III. MODULATION-LINEARIZATION BY FEEDBACK

The basic idea for linearizing the frequency sweep of the varactor tuned Gunn oscillator is shown in Figure 2. A portion of the RF output from the Gunn oscillator is delayed then mixed with an undelayed portion of the RF output. The resulting difference frequency out of the mixer is a function of the rate of change of frequency of the sweep waveform. For a linear ramp of frequency sweep, i.e., constant slope, the difference frequency  $f_B$ , out of the mixer will be a constant. The value of  $f_B$  is determined by the rate of change of frequency and the time delay introduced by the delay device.

$$f_B = (\text{slope})(\text{time delay})$$

$$= \left(\frac{df}{dt}\right) (\Delta t)$$

However, the slope of the output frequency versus modulating voltage is not linear for practical devices; therefore,  $f_B$  will be variable over some range. It is this variable frequency which will be used to generate a correcting signal, which when summed with the ramp voltage and applied to the varactor, produces a more linear frequency sweep. This scheme is a negative feedback system, but it must be realized that instabilities are present throughout the system which could cause the system to go into oscillation under various conditions.



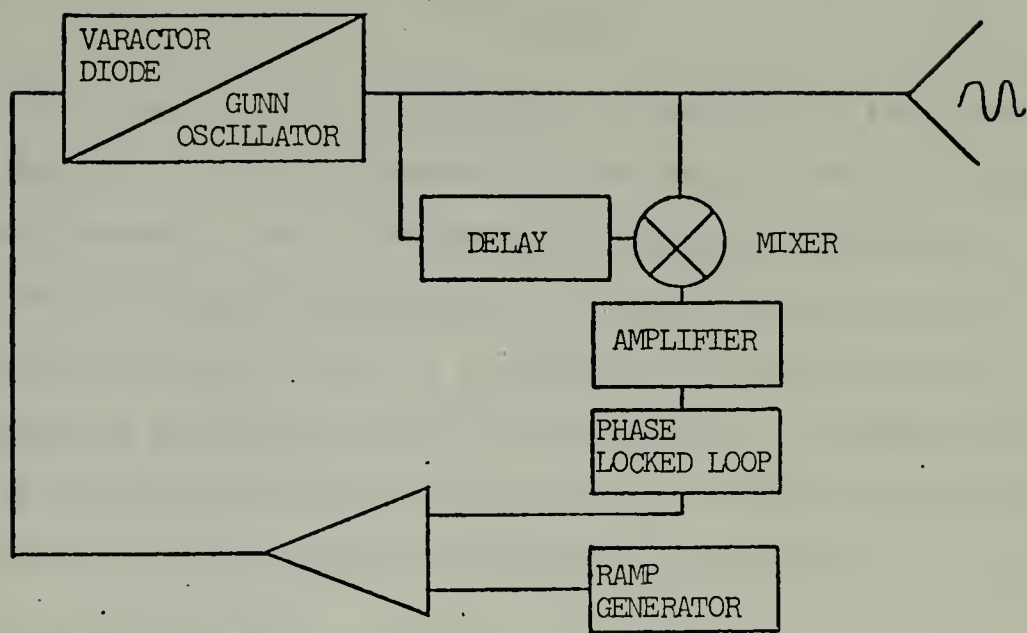


FIGURE 2. Block diagram of basic feedback system



#### IV. DELAY

The first problem encountered in setting up the system was how to obtain the necessary time delay. The delay must be sufficiently long such that the resulting difference frequency is high in comparison to the frequency of the modulation sweep. This is a necessary condition which allows for an ample number of corrections to be made during the period of the modulation sweep. The delay must also be constant over the entire bandwidth of operation.

##### A. TWO METHODS FOR CREATING DELAY

Two possible methods were investigated which could create the delay: 1) coaxial cable, and 2) a microwave acoustic delay device. A third possibility, creating the delay by propagation through a waveguide, was entirely ruled out as being infinitely impractical for this application because of its bulk and high cost.

##### 1. Delay Using Coaxial Cable

For coaxial cable, the velocity of propagation is given by the expression:

$$v = \frac{1}{\sqrt{\mu\epsilon}} = \frac{1}{\sqrt{\mu_r\mu_o\epsilon_r\epsilon_o}} = \frac{c}{\sqrt{\mu_r\epsilon_r}}$$



where:  $c$  = speed of light, approximately  
 $3 \times 10^8$  m/sec

$\mu_r$  = relative permeability, approximately 1.0

$\mu_o$  = permeability constant  
 $= 4\pi \times 10^{-7}$  weber/amp-m

$\epsilon_r$  = relative dielectric constant

$\epsilon_o$  = permittivity constant  $= 8.854 \times 10^{-12}$  F/m

therefore, 
$$v = \frac{c}{\sqrt{\epsilon_r}}$$

When the above expression is applied to the solid dielectric coax such as RG-213, with a relative dielectric constant of 2.3, and loss equal to 47 dB per 100 feet at 10 GHz, the following results:

<u>RG-213</u>		
<u>DELAY</u>	<u>CABLE LENGTH</u>	<u>LOSS</u>
0.1 $\mu$ sec	19.7 meters	30.6 dB
1.0 $\mu$ sec	197 meters	306 dB

Since a delay in the order of 1.0  $\mu$ sec is necessary to give an adequate difference frequency, it is evident that the RG-213 coaxial cable will not be suitable because of its high loss. This loss is much too high for use in a system designed for operation in the milliwatt power range.





Even the lowest-loss cable gives unacceptably high attenuation for a 1.0  $\mu$ sec delay. The lowest loss cable listed in [4] is RG-263 with a solid polytetraflouroethylene dielectric, relative dielectric constant of 1.5 and loss equal to 9 dB per 100 feet. Loss versus length at 10 GHz is as follows:

<u>RG-263</u>		
<u>DELAY</u>	<u>CABLE LENGTH</u>	<u>LOSS</u>
0.1 sec	24 meters	7.1 dB
1.0 sec	240 meters	71 dB

The only acceptable case is the RG-263 with a short delay.

The idea of using coaxial cable to obtain a delay at microwave frequencies is only intended for experimental purposes. It would be illogical to design a miniature radar requiring several hundred feet of bulky coaxial cable for the sole purpose of creating a delay.

## 2. Delay Using MAD Line

The development in microwave acoustic devices has made possible the miniaturization of microwave delay lines. This miniaturization allows the delay line to become an integral part of the radar, making it in this respect ideal for use in the small portable type radar under study. The major problem in using microwave acoustic delay (MAD) lines is their very high attenuation loss, typically 55 dB for a



1.0  $\mu$ sec delay at X band. Yet, the high loss associated with the MAD lines is still lower than that from low-loss coaxial cable for the same delay. Since the MAD line offers small size and relatively low loss, it was chosen as the means of creating the delay.

a. Description of MAD Device Used

The device used had a delay of 1.0  $\mu$ sec, constant over a 2 GHz bandwidth, and produced an attenuation loss of approximately 54 dB at the system operating frequency of 9.5 GHz. The device was very conveniently packaged as can be seen from a photograph of the device with accompanying isolators, Figure 3. The isolators were matched to the device by Teledyne MEC for the purpose of minimizing reflection problems. Configuration of the MAD device as received from Teledyne made its application within the system very easy. The device performed exactly to specifications, producing a 1.0  $\mu$ sec delay over the required frequency bandwidth. Since the delay device was capable of handling 200 mW of average power, no problems were encountered in this respect.



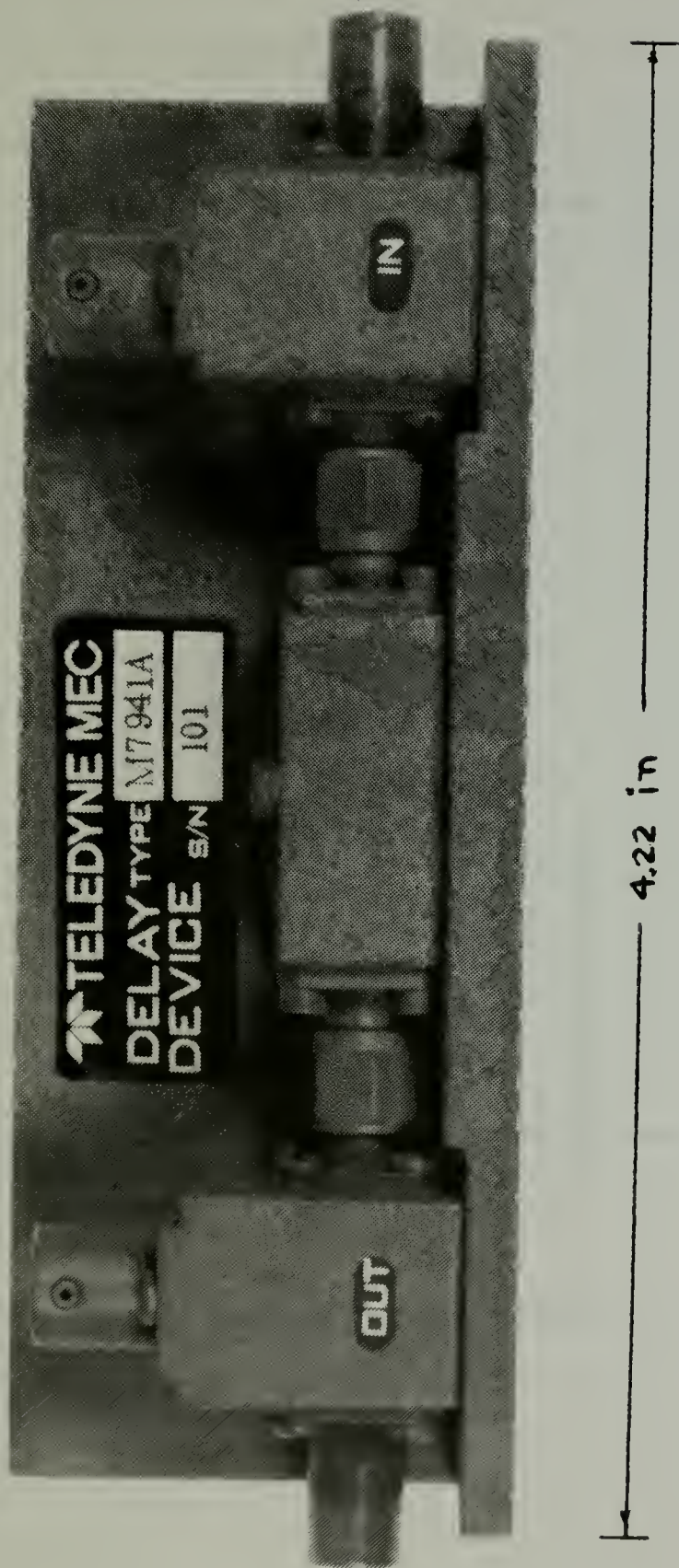


FIGURE 3. Microwave acoustic delay device with isolators attached to input and output ports. Note scale for actual size



## V. SYSTEM PARAMETERS

The portable radar was designed around a center frequency,  $f_0$ , of approximately 9.5 GHz, a maximum range  $R_{\max}$  equal to 5 miles and a ramp (sawtooth) frequency swept waveform as shown in Figure 4.

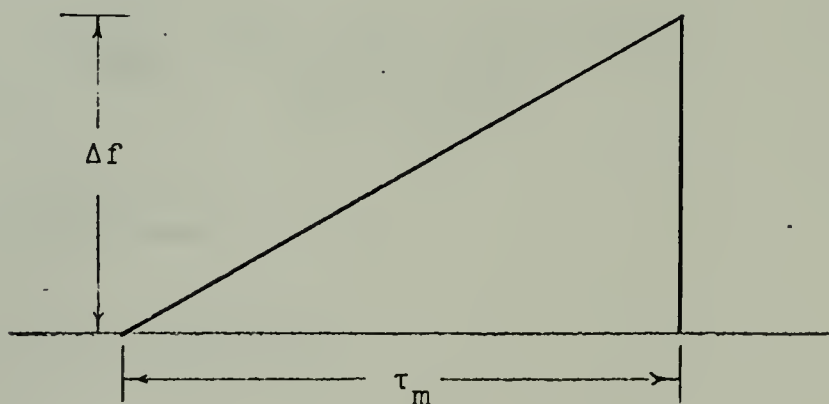


FIGURE 4. Shape of frequency swept waveform





## A. MODULATION FREQUENCY AND PERIOD

Restrictions on the value of the ramp period,  $\tau_m$ , can be found as follows:

$$\text{Velocity} = \frac{\text{distance}}{\text{time}} \quad \text{or} \quad v = \frac{d}{t}$$

Utilizing the above equation with velocity equal to the velocity of electromagnetic propagation  $c$ , the distance equal to twice the maximum range  $2R_{\max}$  to allow the necessary time for electromagnetic energy to transit the  $R_{\max}$  distance and return, and time equal to one-half of the modulation period  $\tau_m$  (the reason for using the factor one-half  $\tau_m$  is explained later in this section), the following results for a range of 5 miles:

$$\frac{1}{2} \tau_m = \frac{2R_{\max}}{c} = \frac{(2)(5 \text{ miles})(1600 \text{ m/mile})}{(3 \times 10^8 \text{ m/sec})}$$

$$\tau_m = 107 \text{ } \mu\text{sec}$$

$$f_m < \frac{1}{\tau_m} \approx 9.35 \text{ KHz}$$

As a comparison, if  $R_{\max}$  were chosen to be 3 miles,  $\tau_m$  would be equal to 64  $\mu\text{sec}$  and  $f_m$  would be less than 15.6 KHz.

For a system using the sawtooth frequency sweep described above, a brief background on theoretical frequency-modulation performance follows.



## B. STATIONARY TARGET AND RANGE AMBIGUITY

Figure 5 depicts a transmitted signal and a received signal which are mixed together at the radar to obtain the beat frequency as shown in the lower part of the figure.

From the figure:

$$f' = f + \dot{f} t_d \quad \text{where} \quad \dot{f} = \frac{df}{dt}, \quad t_d = \frac{2R}{c}$$

$$f' = f + \left(\frac{2R}{c}\right)\dot{f}$$

$$f' - f = \left(\frac{2R}{c}\right)\dot{f}$$

$$\text{DESIGNATE: Range Frequency, } f_R = \left(\frac{2R}{c}\right)\dot{f}$$

Thus, for a stationary target, the beat frequency or range frequency, is directly proportional to target range [5].

The beat frequency  $f_1$  as shown in Figure 5, is the frequency which corresponds to the actual target range, while frequency  $f_2$  corresponds to false range information. If the radar is designed to distinguish between the two frequencies by tracking the lower of the two, then the false signal will not cause errors for the case depicted. But, if the received signal is from a target farther away,  $f_1$  is increased and  $f_2$  decreased. When the echo signal returns to the radar in a time  $\tau_m/2$ ,  $f_1$  and  $f_2$  are equal, Figure 6. Any target at a greater range will cause  $f_1$  to be larger



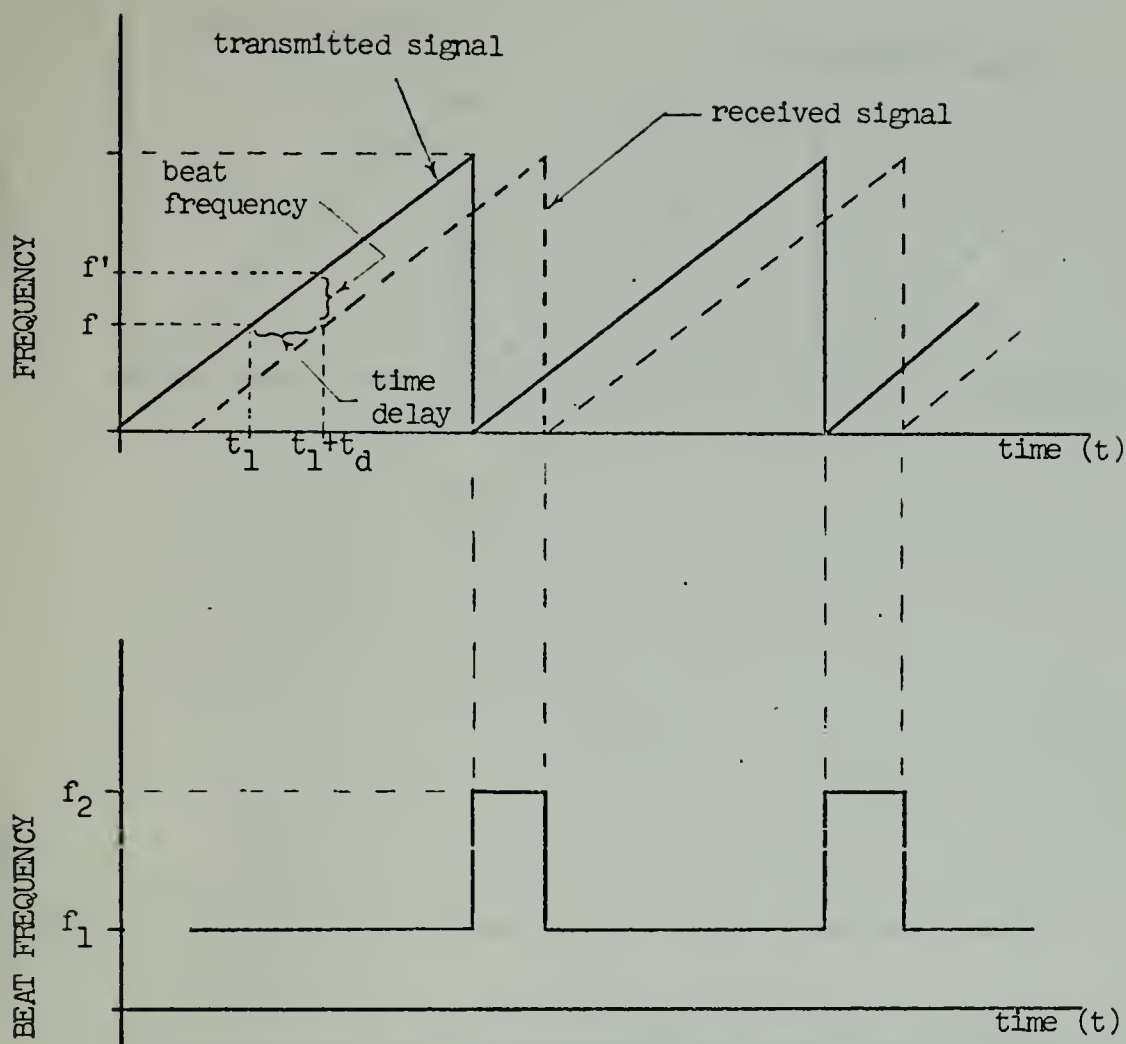


FIGURE 5. Transmitted and received signals from a stationary target at less than maximum range with resulting beat frequency shown below



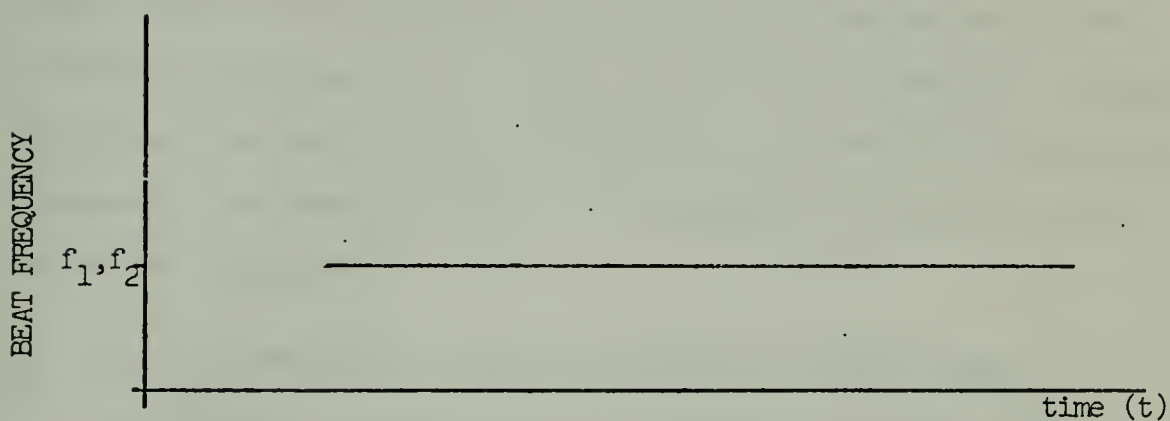
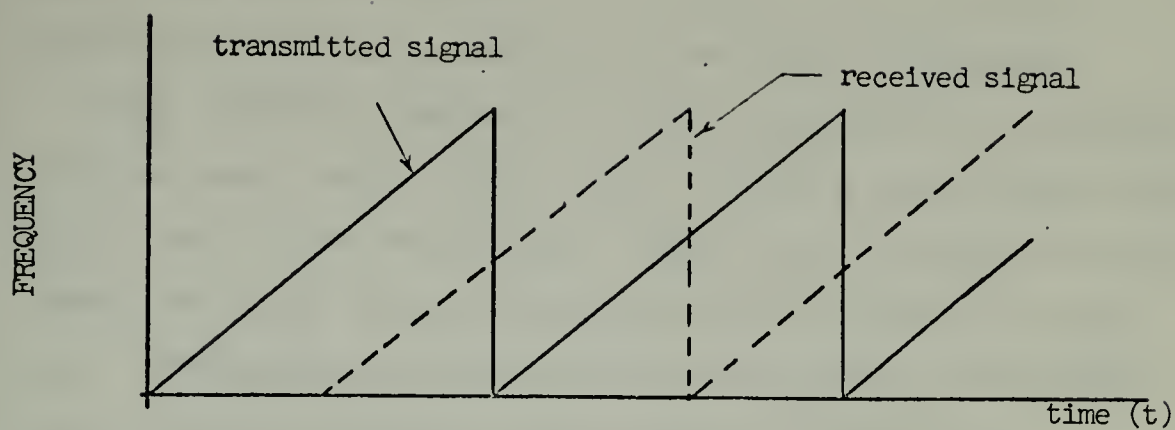


FIGURE 6. Transmitted and received signals from a stationary target at maximum range with resulting beat frequency shown below





than  $f_2$  as shown in Figure 7. If this is the case, the radar would then be presenting false range information.

From the above discussion, range ambiguities are possible when the echo from a target arrives after a time greater than  $\tau_m/2$  since it was transmitted. Thus,  $R_{\max}$  is chosen as that range from which an echo return would be received in time  $\tau_m/2$ . Ambiguities resulting from echo returns from targets beyond designed maximum range could be eliminated by accepting the range frequency only if at the corresponding time, the transmitted frequency is greater than the received frequency. This insures that the echo return is from a target within the designed range capabilities of the radar. A system utilizing this concept would be unacceptably complex for simple portable radar application. It would be much more reasonable to simply accept the ambiguity in the few cases it became applicable.

### C. DOPPLER FREQUENCY SHIFT AND RESULTING RANGE ERROR

When there is relative motion between a target and a radar, it can easily be shown that [6]:

$$f_d = \frac{2v_r}{c} f_o \quad \text{where} \quad \begin{array}{l} v_r = \text{relative velocity between} \\ \text{radar and target} \\ f_o = \text{RF frequency} \\ c = \text{velocity of electromagnetic} \\ \text{propagation} \end{array}$$

Figure 8 shows a transmitted signal, a received signal from a stationary target and a received signal from a moving target.



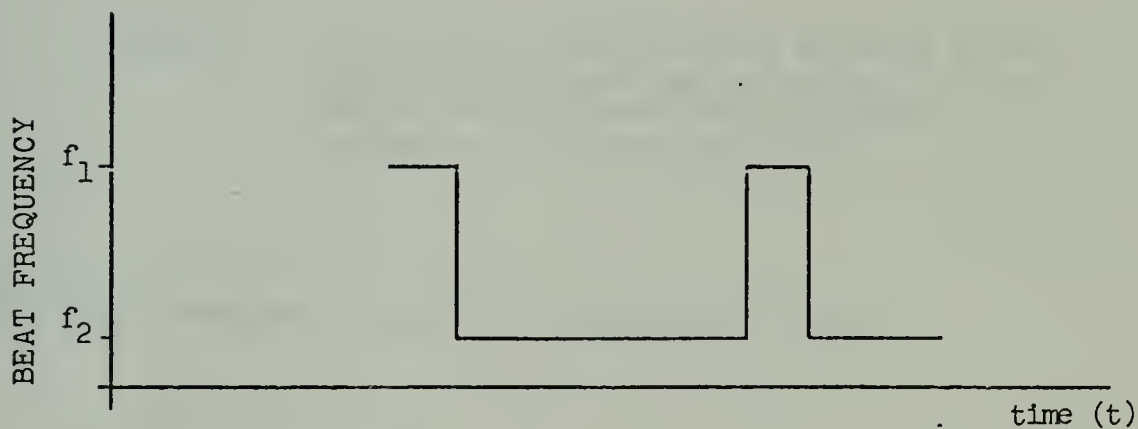
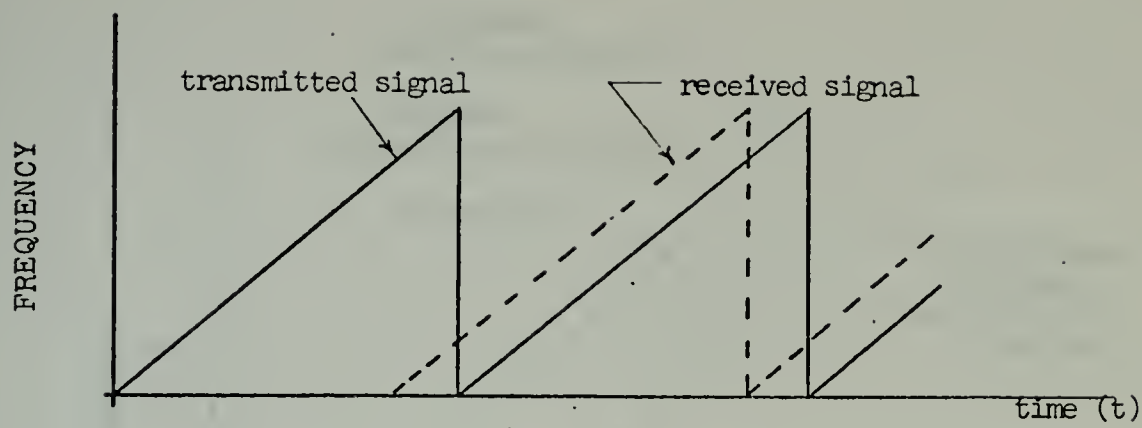


FIGURE 7. Transmitted and received signals from a stationary target at greater than maximum range with resulting beat frequency shown below



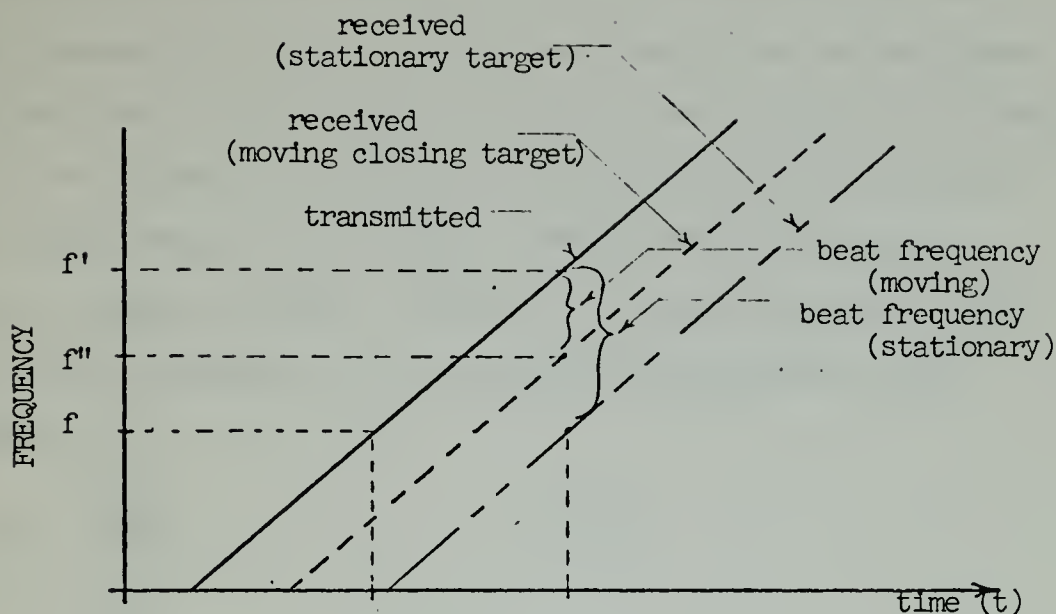


FIGURE 8. Transmitted and received signals from a stationary target and a moving closing target at the same range showing difference in beat frequency

The beat frequency caused by the moving target is:

$$\begin{aligned}
 f_B &= f' - f'' \\
 &= \left[ f + \left( \frac{2R}{c} \right) \dot{f} \right] - \left[ f + \left( \frac{2v_r}{c} \right) f \right] \\
 &= \left( \frac{2R}{c} \right) \dot{f} - \left( \frac{2v_r}{c} \right) f \\
 &\quad \text{range frequency} \quad \quad \quad \text{speed frequency}
 \end{aligned}$$

DESIGNATE: Speed frequency,  $f_S = \pm \left( \frac{2v_r}{c} \right) f$



It should be noted that the sign associated with the speed frequency is (+) if target and radar are moving apart relatively and (-) if target and radar are closing relatively.

It is evident that the beat frequency obtained depends both on the range to the target and the relative speed between target and radar platform. A determination of the range error associated with the doppler-frequency shift follows:

$$f_R = \left(\frac{2R}{c}\right)\dot{f} \quad \text{or} \quad R = \frac{cf_R}{2\dot{f}}$$

$$f_d = \left(\frac{2v_r}{c}\right)f_o$$

The FM radar range to a moving target at a distance R consists of the range associated with a stationary target at the same distance R, plus or minus a range error  $\Delta R$ , associated with the doppler-frequency shift.

$$R + \Delta R = \frac{cf_R}{2\dot{f}} \pm \frac{cf_d}{2\dot{f}}$$

If the expression for  $f_d$  is substituted into the above expression the results are:

$$R + \Delta R = \frac{cf_R}{2\dot{f}} \pm v_r \frac{f_o}{\dot{f}}$$

Therefore, the range error  $\Delta R = v_r \frac{f_o}{\dot{f}}$





To determine the extent of the range error caused by the doppler-frequency shift, a hypothetical case where the relative speed between two craft was 120 miles/hour was considered. This is an extreme case for marine radar application and should represent a maximum effect in range error.

$$120 \frac{\text{miles}}{\text{hour}} \approx 52.8 \frac{\text{m}}{\text{sec}}$$

$$\Delta R = v_r \frac{f_o}{f} = \frac{(52.8 \text{ m/sec})(9.5 \text{ GHz})}{\frac{20 \text{ MHz}}{10^7 \text{ } \mu\text{sec}}}$$

$$\Delta R = 2.68 \text{ meters}$$

This small value of range error indicates that the doppler-frequency shift will have negligible effect on the accurate range measuring capability of the system. The percentage effect varies with the range to the target involved. For the example above, a relative velocity of 120 miles/hour, and a range of 1000 meters, gives a percentage change as follows:

$$\frac{2.68}{1000} (100) = .268\%$$

With an error in measured range of less than 1% in 300 meters even under the extreme case depicted above, it was appropriate to neglect the effect of the doppler-frequency shift in the present system.



#### D. RANGE RESOLUTION

$$f_R = \left(\frac{2R}{c}\right) \dot{f} = \left(\frac{2R}{c}\right) \frac{\Delta f}{\tau_m}$$

$$\tau_m f_R = \frac{2R}{c} \Delta f$$

$\tau_m f_R$  = average number of cycles of the beat frequency occurring in the time of one complete modulation cycle ( $\tau_m$ )

Let:  $\Delta N = \tau_m f_R$

$$\Delta N = \left(\frac{2R}{c}\right) \Delta f \quad \text{or} \quad R = \frac{c \Delta N}{2 \Delta f}$$

$$\delta R = \frac{c \delta(\Delta N)}{2 \Delta f} \quad [7]$$

There exists an indefinite borderline for target resolution at  $\delta(\Delta N)$  approximately equal to one complete beat cycle over the modulation period. That is to say if there is approximately one complete cycle variation over the modulation period  $\tau_m$  between the beat frequencies produced by two different targets, then they will be resolved by the radar as two separate targets.

Let:  $\delta(\Delta N) = 1.0$

$$\delta R = \frac{c}{2 \Delta f}$$



The last equation shows that range resolution  $\delta R$  is dependent on the frequency sweep width  $\Delta f$ . The larger the frequency sweep width, the better (lower value for  $\delta R$ ) the range resolution. Values for  $\delta R$  are tabulated below for frequency sweep widths varying from 10 MHz - 100 MHz.

<u><math>\Delta f</math></u>	<u><math>\delta R</math></u>
10 MHz	15 meters
20 MHz	7.5 meters
30 MHz	5.0 meters
60 MHz	2.5 meters
100 MHz	1.5 meters

A  $\Delta f$  of 20 MHz was selected for the present system because it offered a range resolution capable of distinguishing navigational aids, and yet, still represented less than one-fourth of the available  $\Delta f$  of the varactor-tuned Gunn oscillator.

#### E. BEAT FREQUENCY DEPENDENCE ON FREQUENCY-SWEEP BANDWIDTH

When using the delay-line discriminator, the delay must be constant over the entire operating range of the system. The beat frequency  $f_B$  is a function of both the delay time  $t_d$  and the rate of change of frequency  $\frac{df}{dt}$  [8].

$$f_B = \left(\frac{df}{dt}\right)t_d = \left(\frac{\Delta f}{\tau_m}\right)t_d$$



In order to obtain a suitable beat frequency, a proper combination of  $\Delta f$ ,  $\tau_m$  and  $t_d$  is required. Since the modulation period  $\tau_m$  was calculated to be 107  $\mu\text{sec}$  on the basis of maximum range requirements, and the delay device selected produced a fixed delay time  $t_d$  of 1.0  $\mu\text{sec}$ , then from the above expression, the beat frequency was directly dependent on the frequency-sweep bandwidth  $\Delta f$ .

The choice of a proper  $\Delta f$  was based on the following analysis: With the receiver blanked for the first half of the transmitted sweep, the received signal would be present for a time  $\tau_m/2$  in the receiver. This time was designated  $t_R$  and is approximately equal to  $1/BW$ , where  $BW$  is the 3dB bandwidth of the signal in the i-f amplifier. The 3dB signal bandwidth determines the range discrimination since the difference frequency for a target is directly proportional to its range. Anything that increases the signal bandwidth from a target causes a loss in range discrimination capability. Non-linear frequency modulation of the transmitted signal is one effect leading to this increased bandwidth. The approximation that the increased bandwidth created by errors in the frequency modulation of the transmitted signal is approximately the same as the corresponding increase in beat frequency was used in the analysis.

In the analysis of an FM-CW ranging system [9], it was stated that the separation between beat frequencies of two targets must exceed  $\frac{1}{\tau_m - \tau}$  Hz ( $\tau_m$  is the sweep duration and  $\tau = 2R/c$ ) before the positions of the individual targets





become clearly defined. This expression with  $\tau = \frac{2R_{\max}}{c}$ , where  $R_{\max}$  is 5 miles, results in the approximation of  $t_R = \tau_m/2$  used above.

The concept of the above discussion is developed as follows:

$$f_B = \left(\frac{df}{dt}\right)(t_d) = \left(\frac{df}{dt}\right) \frac{2R}{c}$$

$$\Delta f_B = \frac{2R}{c} \Delta\left(\frac{df}{dt}\right)$$

$$\text{or} \quad \Delta\left(\frac{df}{dt}\right) = \frac{c}{2R} \Delta f_B$$

$$\frac{\Delta\left(\frac{df}{dt}\right)}{\left(\frac{df}{dt}\right)_{\text{avg}}} = \frac{\frac{c}{2R} \Delta f_B}{\left(\frac{\Delta f}{\tau_m}\right)} \quad (100\%)$$

The above equation expresses the percentage deviation of the slope of the output frequency sweep as compared to the average slope ( $\Delta f/\tau_m$ ). The permissible deviation of  $df/dt$  from the average is range dependent with a larger range requiring a smaller deviation of the slope.

If the bandwidth was changed by errors in the frequency modulation of the transmitted signal by an amount for example of 7 KHz, about one-third of the i-f signal bandwidth, then  $\Delta f_B = 7$  KHz, and the expression for the percentage deviation of the slope becomes:



$$\frac{\Delta\left(\frac{df}{dt}\right)}{\left(\frac{df}{dt}\right)_{\text{avg}}} = \frac{\left(\frac{164 \times 10^6 \text{ yds/sec}}{164 \text{ yds}}\right) (7 \text{ KHz}) (100\%)}{\left(\frac{\Delta f}{107 \text{ } \mu\text{sec}}\right)}$$

where:  $R = R_{\text{min}} = 82 \text{ yds for convenience}$   
 $\tau_m = 107 \text{ } \mu\text{sec}$   
 $c = 164 \times 10^6 \text{ yds/sec}$   
 $\Delta f_B = 7 \text{ KHz}$

$$\frac{\Delta\left(\frac{df}{dt}\right)}{\left(\frac{df}{dt}\right)_{\text{avg}}} = \frac{75 \text{ MHz}}{\Delta f}$$

Since  $\Delta f$  was selected as 20 MHz, the permissible percentage deviation of the slope is 3.75%.

Maximum deviation of the slope from the average was determined in order to calculate the required number of corrections that must be applied to maintain a deviation from linearity less than a required amount. From measurements on an uncorrected frequency sweep curve, it was found that the slope at the beginning of the 20 MHz sweep deviated from the average by 37.5% and the slope at the end of the sweep deviated by 17.5% from the average. The average slope being that which would be obtained providing the frequency sweep was perfectly linear. The number of corrections which must be made to the system depends on the worse-case deviation (i.e., 37.5% deviation over half of the modulation period, 53.5  $\mu\text{sec}$ ) and the deviation desired. If for example, the



slope is allowed to deviate by as much as 5% at any instant of time, then this would require approximately 8 or more corrections over the 50  $\mu$ sec time period (i.e.,  $37.5\%/\# \text{ cor.} = 5\% \rightarrow \# \text{ cor.} \geq 7.5$ ). This results in a beat frequency requirement of greater than 160 KHz.

For the system parameters  $\Delta f = 20$  MHz,  $t_d = 1.0$   $\mu$ sec,  $\tau_m = 107$   $\mu$ sec and  $f_B = 187$  KHz, the following results:

$$f_B = 187 \text{ KHz} \quad \text{or} \quad \tau_B = 5.35 \text{ } \mu\text{sec}$$

$$\tau_B = \frac{\frac{\tau_m}{2}}{\# \text{ cor.}}$$

$$\# \text{ cor.} = \frac{\frac{\tau_m}{2}}{\tau_B} = \frac{53.5 \text{ } \mu\text{sec}}{5.35 \text{ } \mu\text{sec}} = 10$$

$$\frac{37.5\%}{10 \text{ cor.}} = 3.75\% \text{ deviation maximum}$$

Thus, the 10 corrections in  $\tau_m/2$  or 20 corrections in  $\tau_m$  resulting from a beat frequency of 187 KHz, provide a sufficient number of corrections to the frequency sweep to reduce the linearization errors to approximately 4%. The above is true providing the correcting circuit works perfectly as designed.



## VI. DETERMINING LINEARITY

Some method is required for measuring the frequency modulation linearity. A point-by-point plot of output frequency versus varactor voltage (time) can be obtained by applying specific voltages on the varactor and monitoring the corresponding output frequencies. A plot of this type is shown in Figure 1 for the device used in this work. However, the point-by-point plot does not give either a continuous nor a dynamic representation.

Two different methods were used to determine dynamically the linearity of frequency-modulation: 1) the tuned cavity and probe method, and 2) the beat-frequency method.

### A. TUNED CAVITY AND PROBE METHOD

Some method for observing the output in the form of a continuous plot of frequency versus time on an oscilloscope is desirable. This method offers the advantages of being able to view and to record easily the output waveshape (i.e., output frequency versus time), and to detect changes in waveshape while varying parameters. To obtain an oscilloscope display, a frequency discriminator is required. A discriminator was constructed using a tuned cavity with probe and crystal detector. The basic idea is to use the variation of impedance with frequency on a resonant peak near the physical center of the cavity [10]. The cavity section is coupled to the main guide through an inductive





iris. Its resonant frequency can be varied by means of an adjustable short. Figure 9 illustrates this apparatus. The probe depth is varied to obtain the maximum coupled signal on the oscilloscope while the sliding short is varied to obtain an output voltage proportional to frequency.

### 1. Cavity Linearity

The cavity utilized was a standard waveguide section cut to length for resonance in the  $TE_{103}$  mode at X-band. The resonance frequency was made alterable by means of the adjustable short which was tuned until a good linear portion of the slope of a resonant peak was obtained.

Since the frequency sweep is only 20 MHz while the center frequency is approximately 9.5 GHz, the frequency sweep represents a very small change in frequency when compared to the center frequency, i.e.,  
 $(20 \text{ MHz} / 9.5 \text{ GHz}) (100) \approx 0.2\%$ .

Cavity  $Q$  can be calculated by the expression  $Q = f_0 / \Delta f$ , where  $f_0$  is the center resonant frequency of the cavity and  $\Delta f$  is the 3 dB frequency bandwidth, see Figure 10. For  $f_0$  equal to 9.5 GHz and  $\Delta f$  approximately 40 MHz, the cavity  $Q$  is around 240. Then it is a reasonable assumption that cavities with  $Q$ 's lower than 200 would exhibit linear regions over a 20 MHz frequency band on the slope of the resonant peak. It is reasoned that a lower  $Q$  cavity would be more desirable since a larger linear



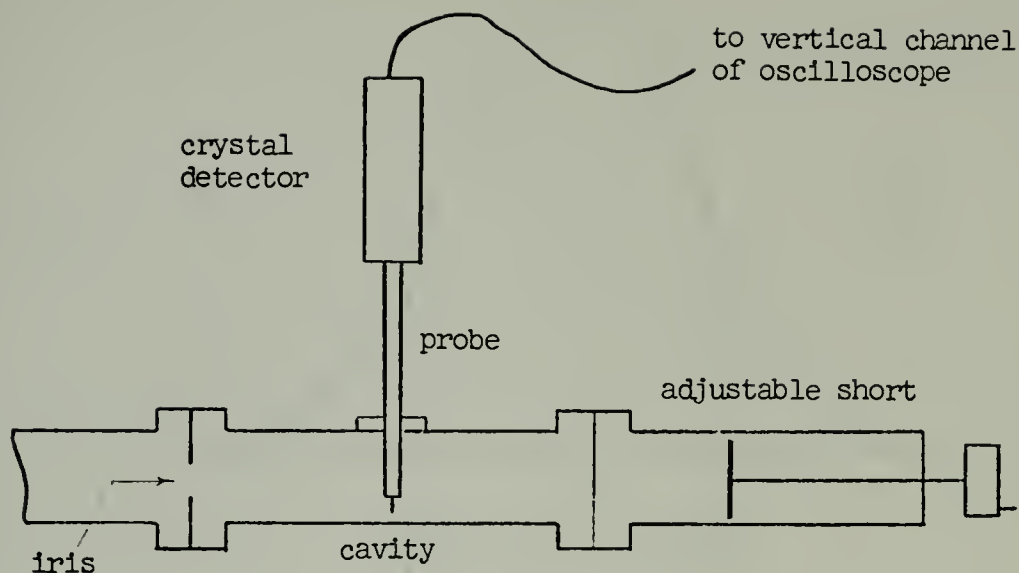


FIGURE 9. Cavity and probe apparatus

portion could be utilized. The ability to utilize the large linear portion of a lower  $Q$  cavity reduces the possibility of waveform distortion caused by operation off of the linear portion of the resonant slope.

## 2. Probe/Diode Detector Linearity

A questionable area involving linearity when using this method is whether or not the diode detector is actually linear over the region of interest. To determine whether or not the diode detector is linear, the probe was first inserted in the cavity and data was taken to determine the



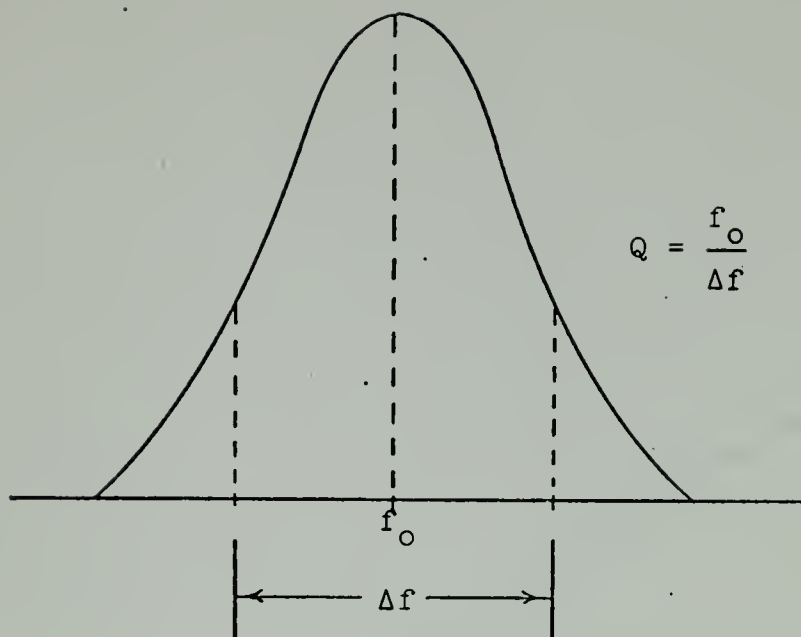


FIGURE 10. Resonant peak showing  $f_0$  and  $\Delta f$

range of output voltages as the varactor voltage level was changed through its entire range. Then the diode detector was removed from the assembly, and a modulated source was fed through an attenuator directly to the input of the detector. The input level was changed through a range which caused the output voltage from the diode detector to change through the full range of interest.

Figure 11 is a plot of diode detector output voltage versus the varactor voltage. This establishes the range of output voltage over which the diode detector linearity is



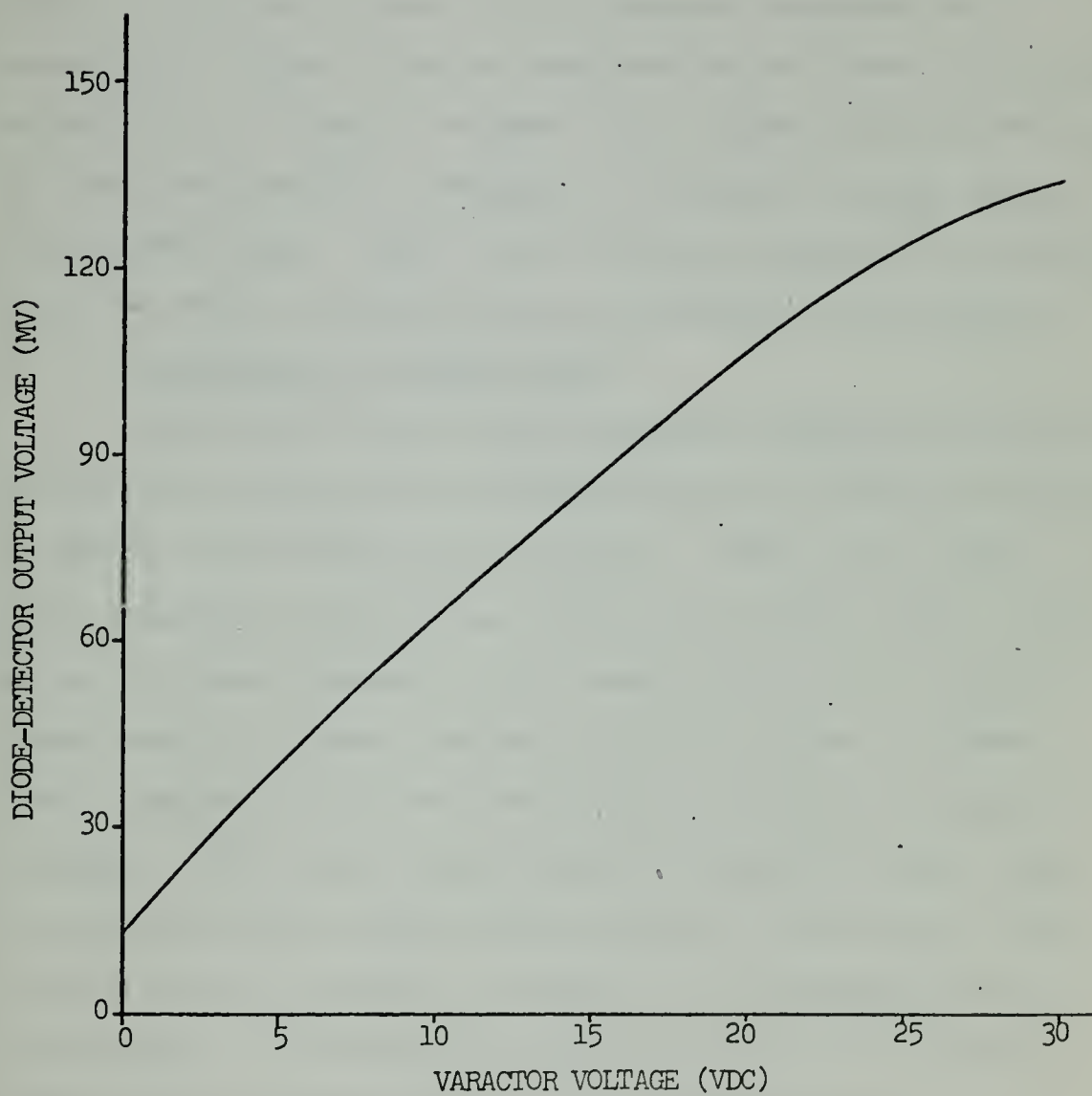


FIGURE 11. Diode-detector output voltage versus varactor voltage





in question. Figure 12 shows the output voltage of the diode detector as the input was varied over a range sufficiently large to establish the same range in output voltage as obtained from Figure 11. Form a comparative check of the two figures, diode detector response was essentially linear from the high end 140 MV, down to approximately 15 MV of output voltage. This linear range corresponds to that obtainable by changing the varactor voltage through its entire range. Thus, diode detector linearity was established over the entire operating range capability of the system.

### 3. Limitations on Cavity Use

The use of the cavity to measure modulation linearity as outlined above presents problems when it becomes necessary to check the linearity very closely. First, the cavity is a power sensitive device which means the voltage output picked up at the probe changes as the power level of the varactor-tuned Gunn oscillator changes (Figure 13 shows the power level changes in the Gunn oscillator as varactor voltage is changed). Therefore, output waveform representations must be compensated for power fluctuations at the source. Also, there exists the problem of being able to determine with any accuracy the degree of linearity of the output wave-shape from its presentation on the oscilloscope.



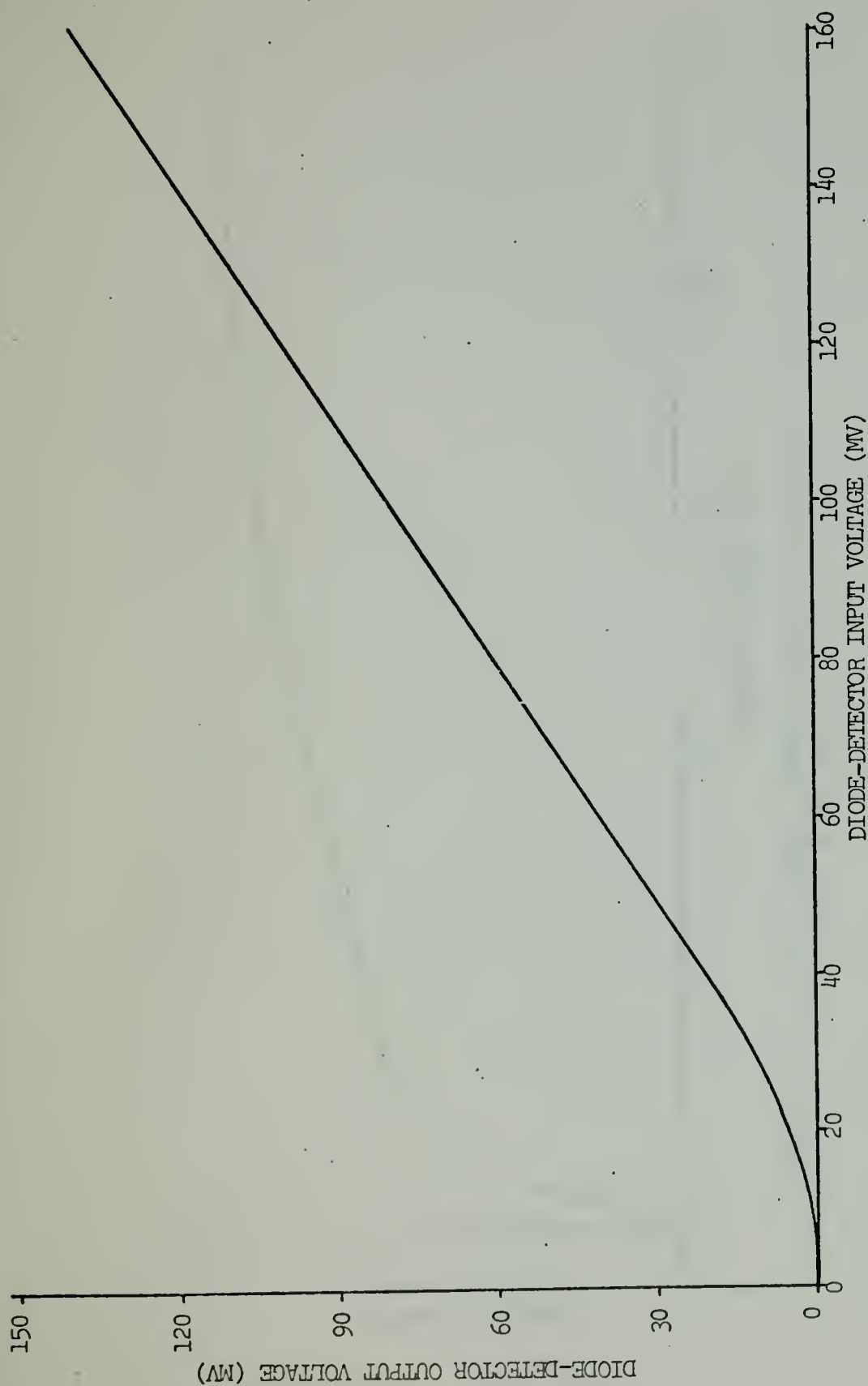


FIGURE 12. Diode-detector output voltage versus diode detector input voltage



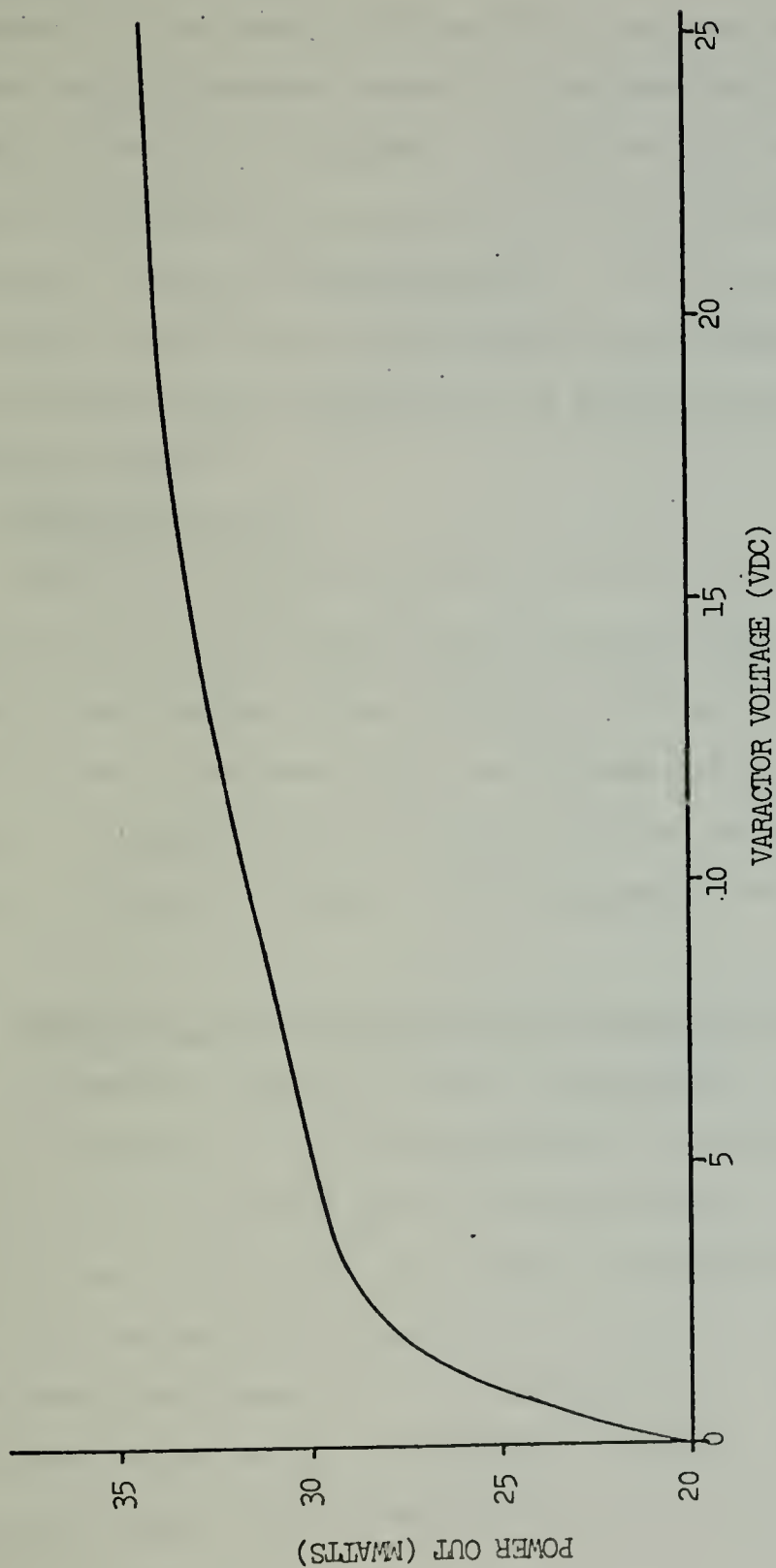


FIGURE 13. Power output versus varactor voltage  
Gunn bias = 10 volts



## B. BEAT-FREQUENCY METHOD

Because of the above problems with the tuned cavity and probe method, another method for determining the degree of linearity was also utilized. In this second method, the delay line and mixer which are part of the linearizing circuit were used as a discriminator. The time between the peak of each cycle of the beat frequency was determined through the use of an oscilloscope, a pulse generator and a frequency counter.

### 1. Equipment Setup

The beat frequency was fed into one channel of a dual-trace oscilloscope while the pulse generator was fed into the other channel. The frequency counter was synchronized with the pulse generator, and consequently, it displayed the pulse repetition rate selected on the pulse generator. Figure 14 shows a block diagram of this equipment setup.

### 2. Measuring Time Between Beat-Frequency Peaks

To measure the time between consecutive peaks of the beat frequency it was only necessary to adjust the pulse generator repetition rate such that the second pulse coincided exactly with the first peak of the beat frequency signal, the frequency was read on the counter and repeated for the remaining peaks of the beat frequency. Since the first pulse occurs at the beginning of the beat-frequency signal and remains there throughout all the measurements,





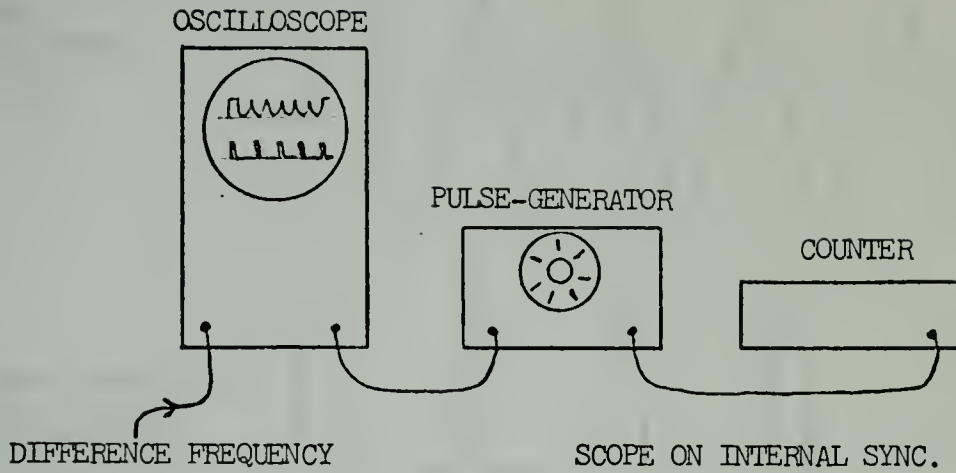
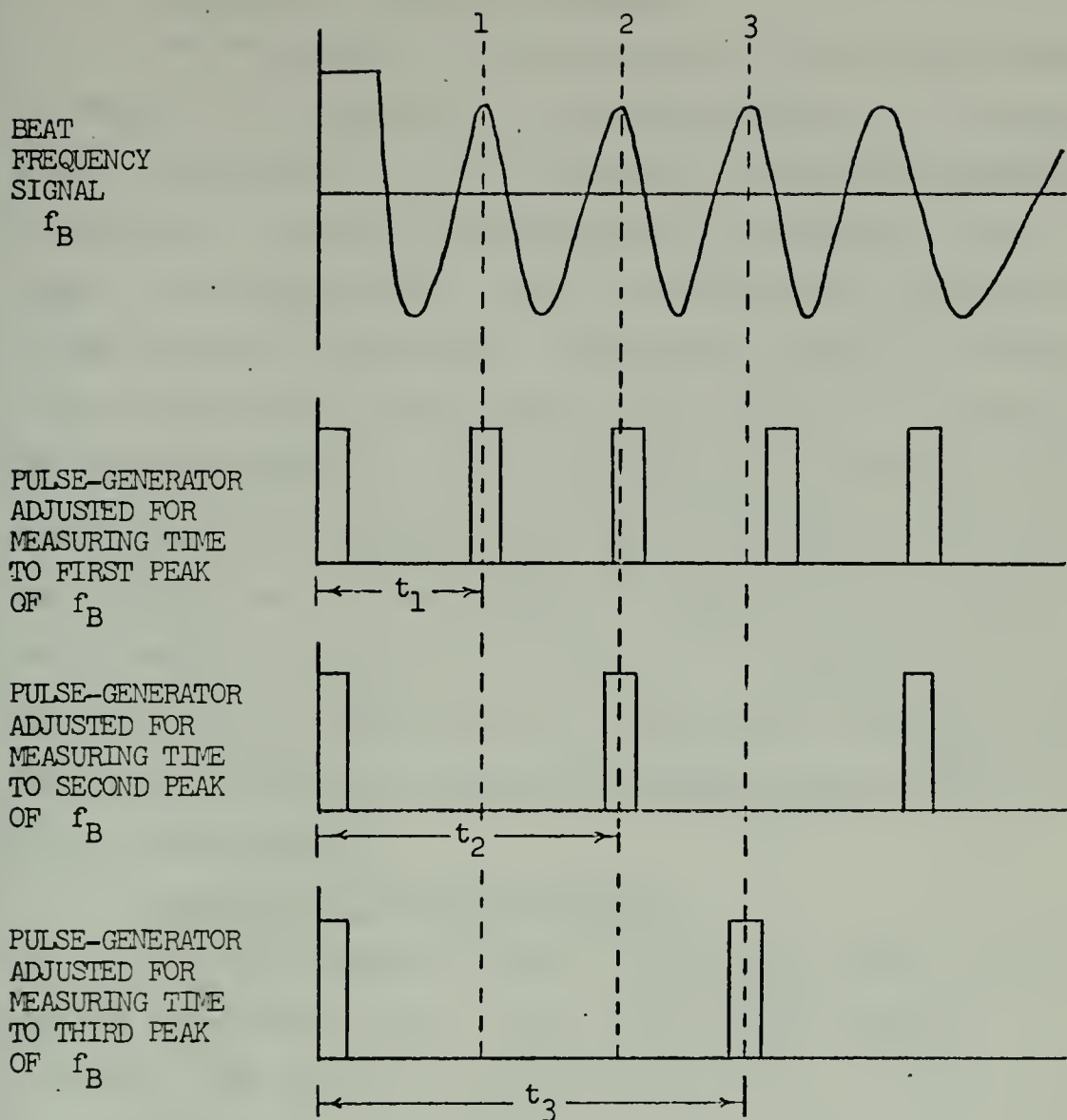


FIGURE 14. Block diagram of equipment setup used for measuring time between peaks of the beat frequency signal

it was strictly utilized as a reference point. This meant that the reciprocal of the frequency read from the counter was representative of the time from the reference point to each of the individual peaks of the beat-frequency signal. To obtain the time between consecutive peaks, it was simply a matter of taking the difference between the time from the reference point to each of the consecutive peaks. This concept is shown diagrammed in Figure 15.





time between 1 and 2

$$t = t_2 - t_1$$

time between 2 and 3

$$t = t_3 - t_2$$

FIGURE 15. Method used for measuring time between beat frequency peaks



### 3. Accuracy in Time Measurements

In the method outlined above, the counter was used to measure the frequency of the pulse generator. It would also be appropriate to use the counter to directly measure the period of the pulse train and make calculations more simple. The determining factor for which to use was governed by the accuracy obtainable. The counter used had resolution of 0.1  $\mu$ sec on the period scale while it had 10 Hz resolution when reading frequency in the KHz range. It was found when this method was attempted, that the best accuracy obtainable was governed not by the counter but rather by the system, and it was on the order of 0.1  $\mu$ sec. This made the use of the period measuring function of the counter more attractive since this eliminated converting frequency measurements to period measurements.

### 4. Meaning of Time Measurements

If the frequency sweep is perfectly linear, the time between consecutive peak values of the beat frequency is a constant. Any deviation from linearity will be evident from the varying times noted between the peak values of the beat frequency. This deviation can be represented as a percent deviation from linearity; therefore, this method offers a more accurate approach to the determination of linearity of the frequency sweep.



## VII. FINAL EQUIPMENT SETUP

A block diagram of the final equipment setup is shown in Figure 16. The 1 mA ammeter was used to monitor the mixing current which was controlled to approximately 1 mA for proper mixing. A Wavetek model 142 HF generator was utilized as a ramp generator. The ramp retrace time associated with this piece of equipment was excessive and produced problems in the correcting system as discussed in Section XI. To minimize adverse effects on the correcting system because of this condition, a simple special purpose ramp generator with a fast retrace could be constructed using a few active devices as described in [11]. Figures 17 and 18 are photographs of the system showing the delay device, mixer, cavity and probe, milliammeter and circuitry. Figures 19 and 20 show closeup views of the correcting circuit and external amplifier, respectively. Figure 21 gives a detailed schematic diagram of the entire correcting circuit between the output of the mixer and the input to the varactor.





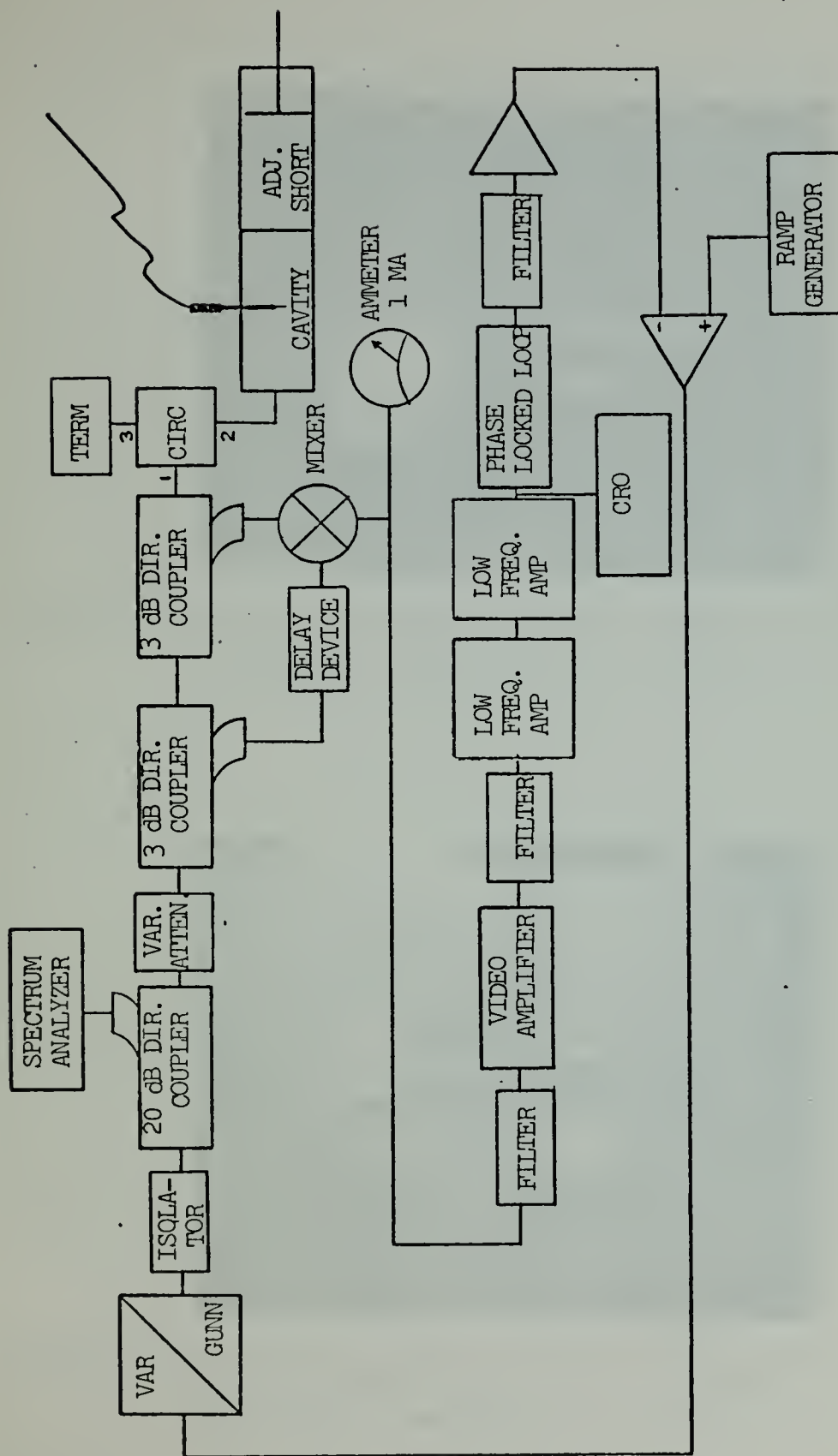


FIGURE 16. Block diagram of final equipment setup



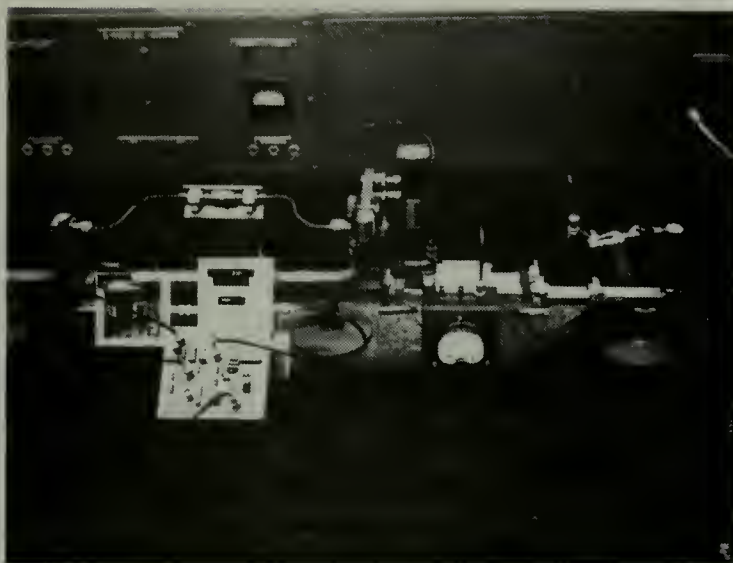


FIGURE 17. Laboratory system assembly showing delay device, mixer, cavity and probe and circuitry. View no. 1.

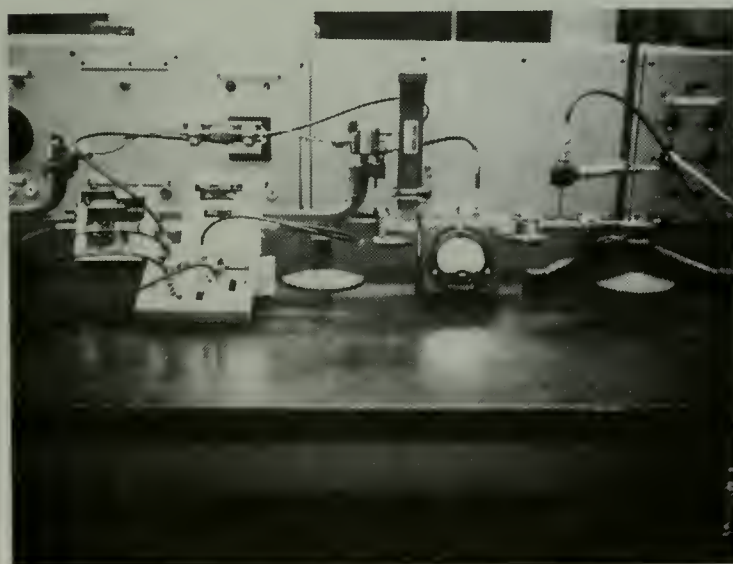


FIGURE 18. Laboratory system assembly showing delay device, mixer, cavity and probe and circuitry. View no. 2.



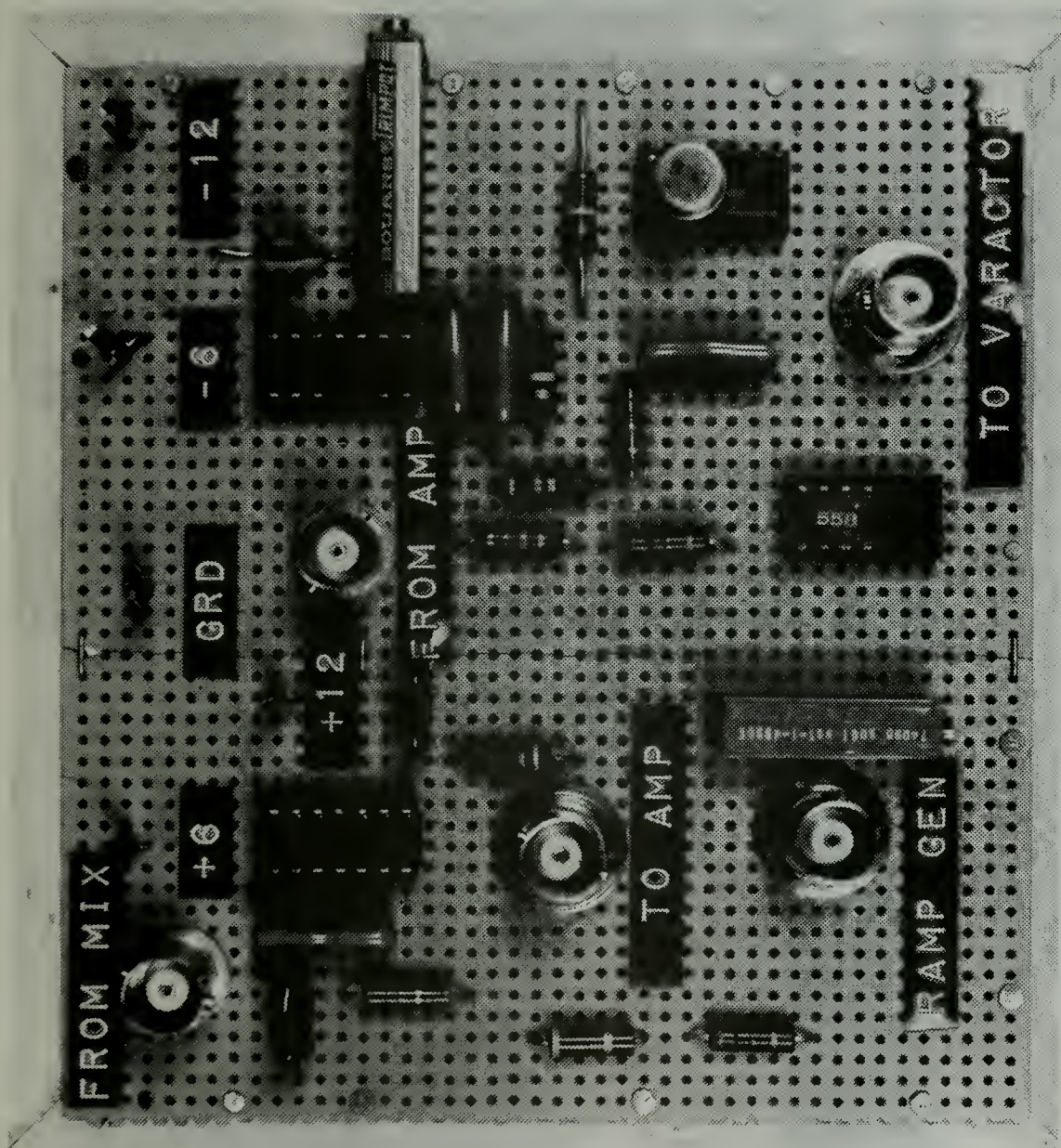


FIGURE 19. Correcting circuit, closeup view





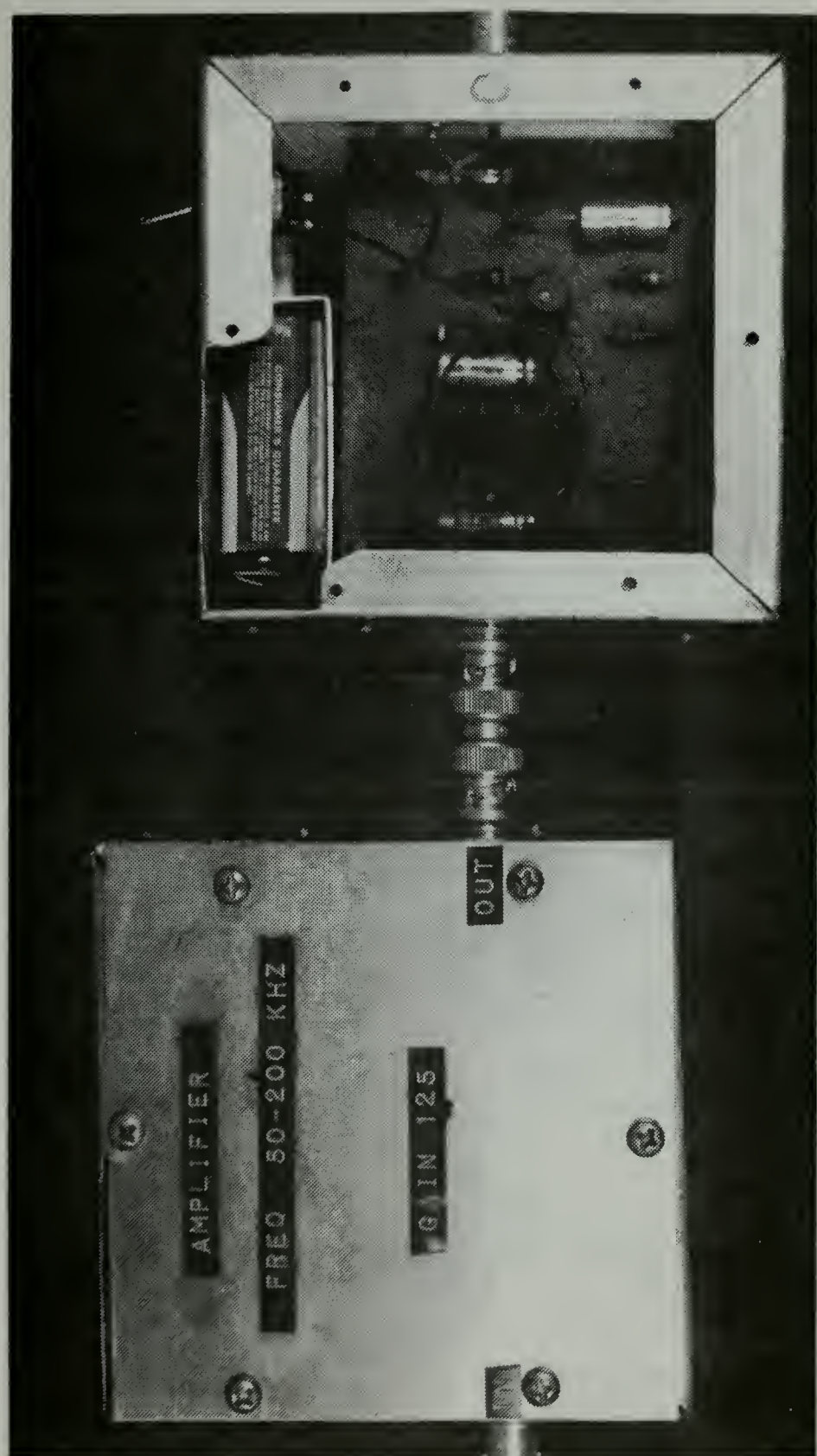
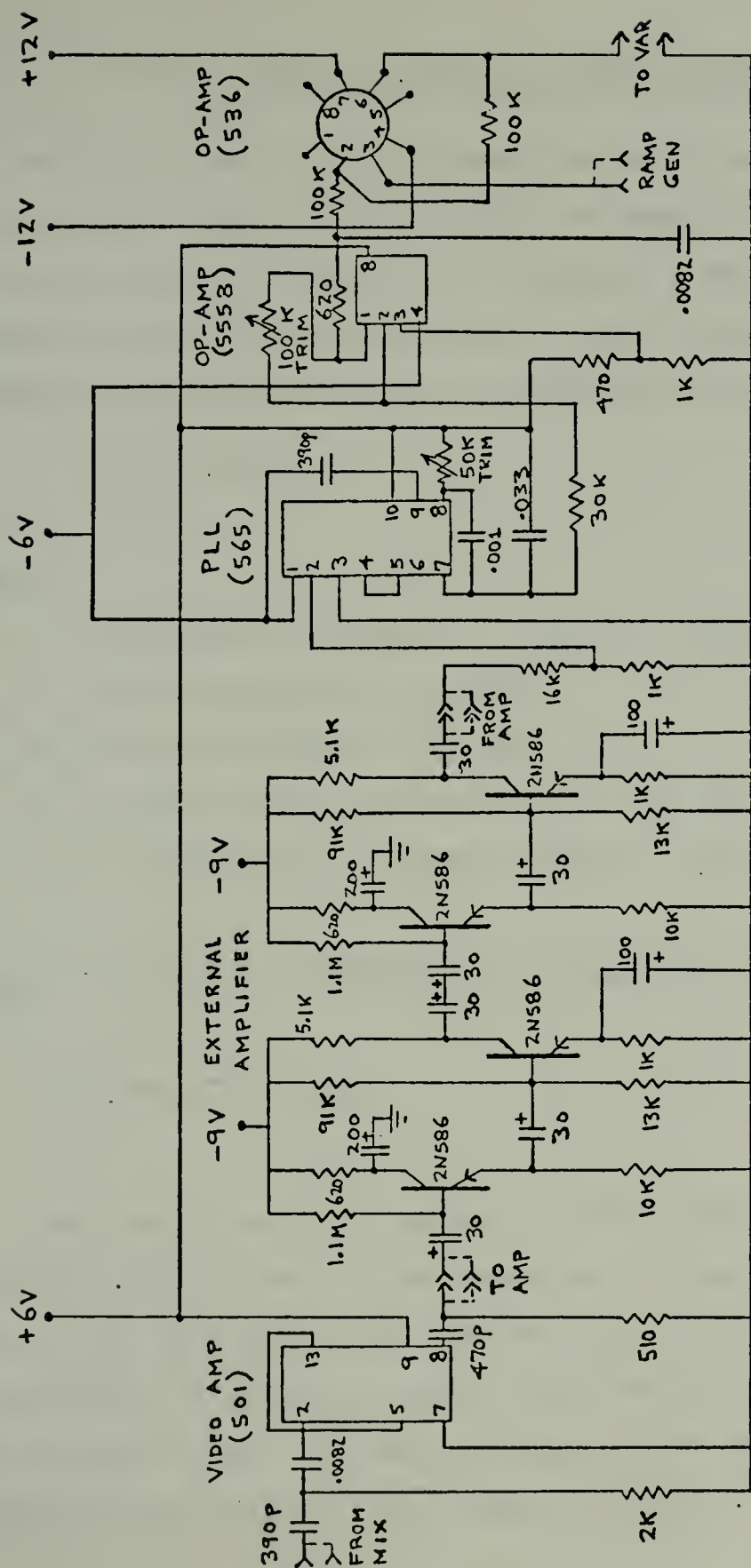


FIGURE 20. External amplifiers, closeup view









### VIII. EFFECT OF NOISE IN CORRECTION CIRCUIT

The first amplifier following the mixer in the final setup is the video amplifier, 501, as shown in Figure 21. At this point in the system, the desired signal is at its minimum value. The following is a brief analysis on the possible effects of noise on the correcting circuitry.

$$N_{out} = kTB_nGF$$

where:

$$k = \text{Boltzman's constant} = 1.38 \times 10^{-23} \text{ Joules-}^\circ\text{K}^{-1}$$

$$T = \text{Room temperature} \approx 300^\circ\text{K}$$

$$B_n = \text{Noise bandwidth} \approx 20 \text{ MHz}$$

$$G = \text{Gain of video amplifier 501: } 25 \text{ dB} = 300$$

$$F_o = \text{Noise figure of video amplifier 501: } 5 \text{ dB} = 3.16$$

$$\begin{aligned} N_{out} &= (1.38 \times 10^{-23} \frac{\text{watt-sec}}{^\circ\text{K}})(300^\circ\text{K})(20 \times 10^6/\text{sec})(300)(3.16) \\ &= 7.87 \times 10^{-10} \text{ watts} \end{aligned}$$

The signal level at the input to the delay device was approximately 15 mW. After traveling through the delay device (55 dB attenuation) and the mixer (5 dB attenuation), the signal at the input to the video amplifier was down 60 dB from 15 mW. The amplifier gain of 25 dB made the signal at the output of the video amplifier 35 dB down from



15 mW, or  $4.74 \times 10^{-6}$  watts. Therefore, noise power is far less than signal power and should not be a problem in circuit operation.



## IX. PHASE-LOCKED LOOP

Phase-locked loops are a class of circuits based on frequency-feedback technology. A phase-locked loop (PLL) consists of a phase detector followed by a low-pass filter and a voltage-controlled oscillator. If the incoming frequency is changing, the phase detector output voltage changes just enough to keep a nearly constant phase difference between the oscillator signal and the incoming signal. In this manner, the PLL has the ability to track or stay locked onto a changing incoming frequency on a cycle for cycle basis. The average "error" voltage applied to the oscillator is a function of the incoming frequency. The low-pass filter voltage is the demodulated output when the signal at the input is frequency modulated. If the oscillator frequency is a linear function of the control voltage, the phase-locked loop can be used as a linear discriminator, with variation in output voltage proportional to change in frequency.

Phase-locked loops can have good noise immunity, easily adjusted center frequency, bandwidth adjustment, high selectivity, high-frequency operation capability and center-frequency tuning by means of a single external component [12].

From the block diagram of a phase-locked loop, Figure 22, with no signal input the error voltage,  $V_{\text{error}}$ , is equal to zero. Under this condition, the voltage-controlled oscillator VCO, operates at its free-running frequency,  $f_0$ .





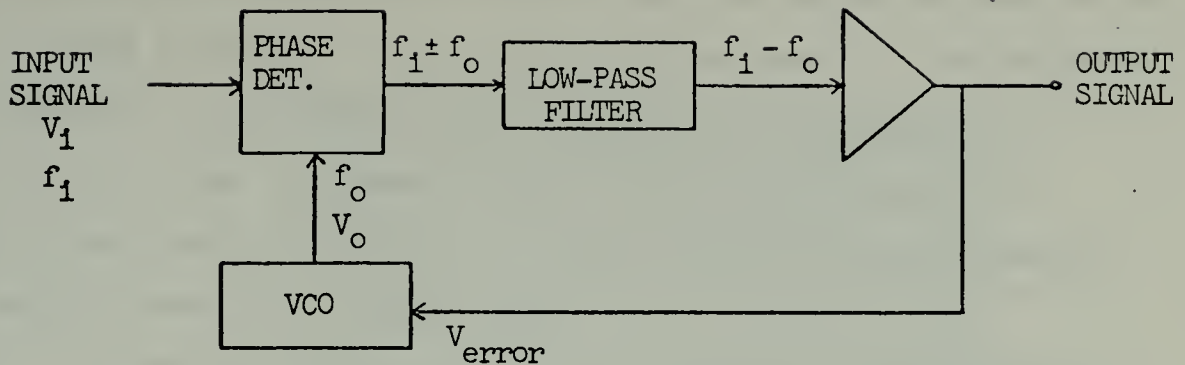


FIGURE 22. Block diagram of phase-locked loop

The free-running frequency is determined by the choice of components used. When an input signal is applied to the PLL, the phase comparator compares the frequency and phase of the input frequency to that of the VCO and generates an error voltage,  $V_{\text{error}}$ , which is related to the phase difference between the signals. The error voltage is filtered, amplified and applied as a control voltage on the VCO. The error voltage forces the VCO to change frequency in the direction that will minimize the phase difference between oscillator and input signal.

The range of frequencies over which the PLL can acquire lock with an incoming signal is called the "capture-range", and the range of frequencies which the PLL can maintain track with an incoming signal is called the "lock-range".



Once the PLL is in lock, the VCO frequency is the same as the incoming signal frequency and the error voltage is dc.

The effects of the low-pass filter are: 1) the capture process becomes slower with increased filtering, 2) the capture range decreases with increased filtering, and 3) the transient response of the loop becomes underdamped with increased filtering [13].

In the application of the PLL for detecting changes in the difference frequency, the input signal to the PLL was the difference frequency while the error voltage,  $V_{\text{error}}$ , was sensed and utilized as a correcting signal for the varactor tuned Gunn oscillator. Optimum filtering was found to be a problem. A lack of filtering caused the error voltage to have a large ripple on it. This ripple voltage frequency modulated the signal by a corresponding amount, with a resulting distorted output waveform. Excessive filtering distorted the correcting signal to the point where it was no longer a "correcting signal", but once optimum filtering was accomplished, the error voltage obtained was clean and practically distortion-free. A photograph of the optimum correcting signal obtained is shown in Figure 23. The limited distortion evident in the correcting signal was because of the delaying effects of filtering and problems involved with the retrace time between successive voltage ramps. These problems are discussed further in Sections X and XI.



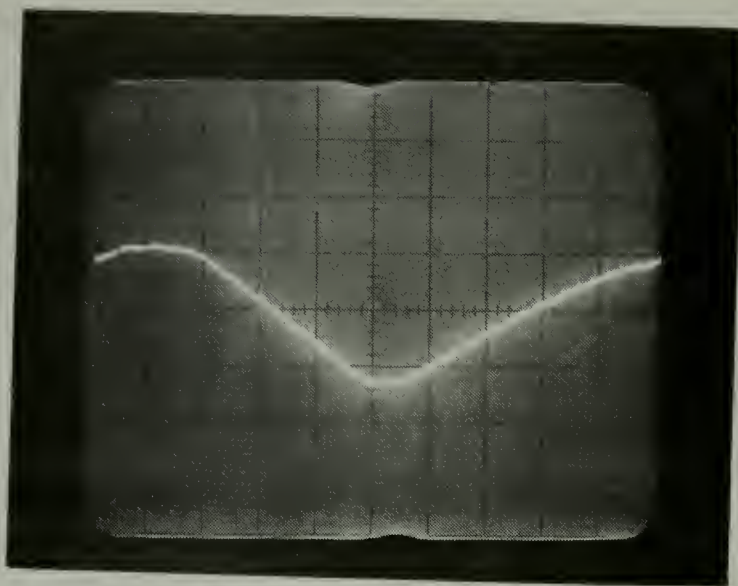


FIGURE 23. Correcting signal (AC) as viewed at  
input to differential amplifier (536)  
Scale: 0.1 volt/division



## X. DELAY AND FILTERING

The basic idea of the system was to detect a nonlinearity in the output frequency sweep, develop a signal to correct for the nonlinearity and apply the correcting signal onto the varactor. This would alter the output frequency in such a manner that the resulting frequency sweep was more linear than before.

An inherent problem in the system was the fact that instantaneous correcting was not possible. A finite delay time existed between the time of detection of the fault and the actual application of the correcting signal. This finite delay time was increased greatly by the addition of filters in the correction loop.

Since the output of the phase-locked loop was somewhat noisy, considerable filtering was required before application of the correcting voltage on the varactor. The filtering was necessary because any ripple voltage riding on the correcting signal caused the output frequency to be modulated by a corresponding amount. Thus, it was essential that a certain amount of filtering be utilized within the closed-loop system.

In contrast, too much filtering distorted the correcting-voltage waveform so badly that rather than correct the nonlinearity, it caused a further deviation from linearity. Optimum filtering was determined by laboratory testing.





## XI. VOLTAGE RAMP RETRACE TIME

The FM-CW radar herein described depends upon a constant rate of change of frequency for its operation. It is therefore necessary to gate off the transmitter or receiver during the frequency retrace time. It is desirable to reduce the retrace time to an absolute minimum in order to maximize the useful average power.

By minimizing the retrace time, not only is the useful average power maximized, but also the time available for correcting the non-linearity in the sweep. This is discussed further in Section XIII.



## XII. OPTIMUM CORRECTING VOLTAGE

The correcting signal which produced optimum linearization of the output-frequency sweep is shown in Figure 23. This signal is shown again in Figures 24 and 25 with the AC portion of the corrected ramp signal to the varactor for one and two cycles of modulation frequency, respectively. In each figure, the distortion in the ramp introduced by the correcting circuit in order to linearize the frequency sweep is clearly evident.

To obtain the optimum correcting voltage, many hours of laboratory measurements were made. A possible optimum signal was selected, then the output-frequency waveform was observed using the cavity and probe technique of Section VI, and the beat-frequency signal was monitored for linearity as also outlined in Section VI. When the optimum signal was found, it was recorded by taking photographs of the output-frequency waveform Figure 27, beat-frequency signal, Figure 29, and the correcting signal, Figure 23, and recording data for plotting the percent deviation from linearity versus time during the modulation sweep Figure 30.

Figure 26 is a photograph of the uncorrected output-frequency waveshape and is shown above that of the corrected output-frequency waveshape Figure 27 for comparison. Upon comparing these two figures, the corrected output-frequency waveshape appears to be much more linear than that of the



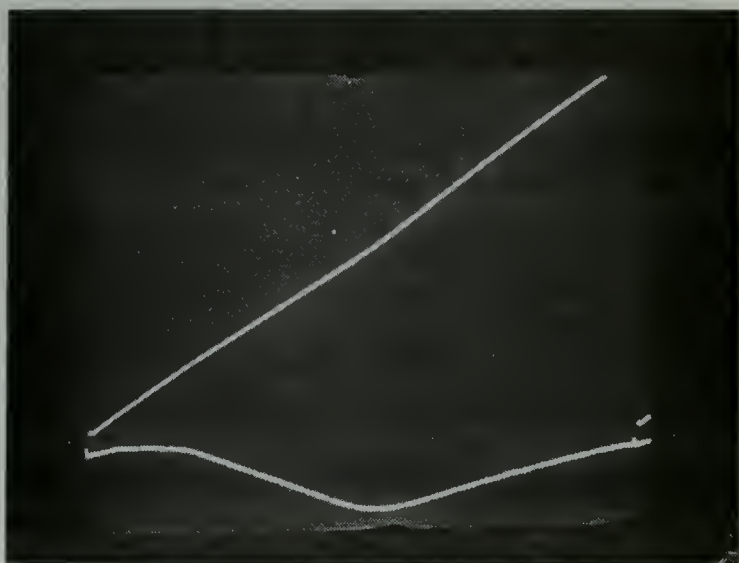


FIGURE 24. Corrected ramp (AC) with correcting signal (AC) shown below.  
Scale: Ramp 1 v/div. cor. sig. .2v/div.

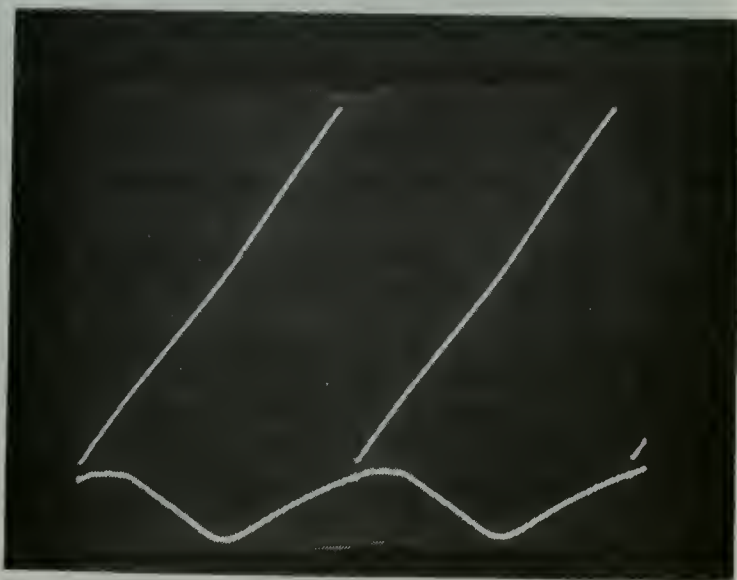


FIGURE 25. Corrected ramp (AC) with correcting signal (AC) shown below for two cycles.  
Scale: Ramp 1 v/div. cor. sig. .2v/div.





FIGURE 26. Uncorrected output frequency waveform as obtained from cavity and probe

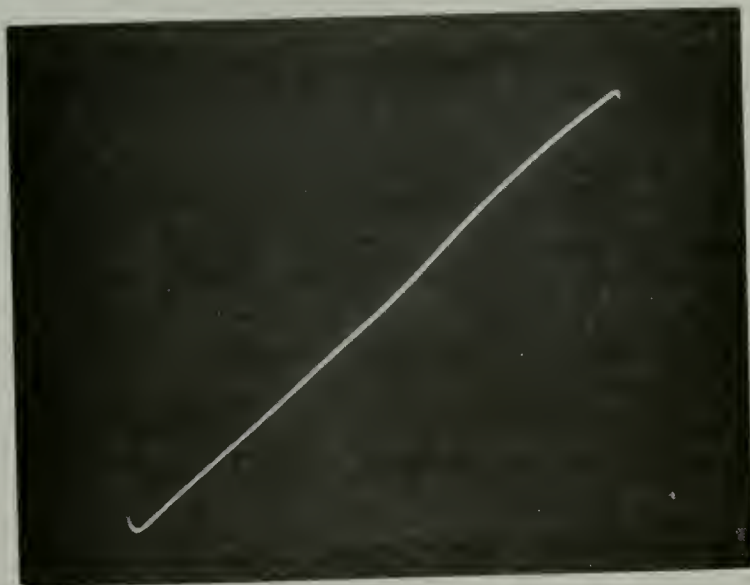


FIGURE 27. Corrected output frequency waveform as obtained from cavity and probe





uncorrected. This comparison even though limited when viewed with the restrictions discussed in Section VI, still represents a significant linearization of the output-frequency sweep. Analyzing the degree of linearization present was difficult using this method. All numerical calculations on the sweep deviation from linearity were based on the beat-frequency method and are presented in Section XIII.



### XIII. LINEARITY ANALYSIS

Figure 28 shows a photograph of the uncorrected beat frequency as recorded at the output of the external amplifier. The peaks of the beat-frequency signal are quite apparent, and the time between successive peaks became larger when proceeding from left to right. This corresponds to a frequency sweep starting with a high slope and ending with a low slope.

Figure 29 shows the beat frequency with the correcting signal applied to the varactor. This photograph shows the much smaller deviation of the period between the peaks of the beat frequency, and represents a more linear frequency sweep.

The beat frequency associated with a perfectly linear slope was 187 KHz for this system. This frequency is based on the average slope of the output-frequency waveform and the delay provided by the delay device. In order to present the recorded data in an acceptable manner, consider the following:

$$f_B = (\text{slope})(\text{time delay})$$

$$= \left(\frac{df}{dt}\right) (\Delta t) \quad \text{where } \Delta t \text{ is a constant } 1.0 \text{ } \mu\text{sec}$$



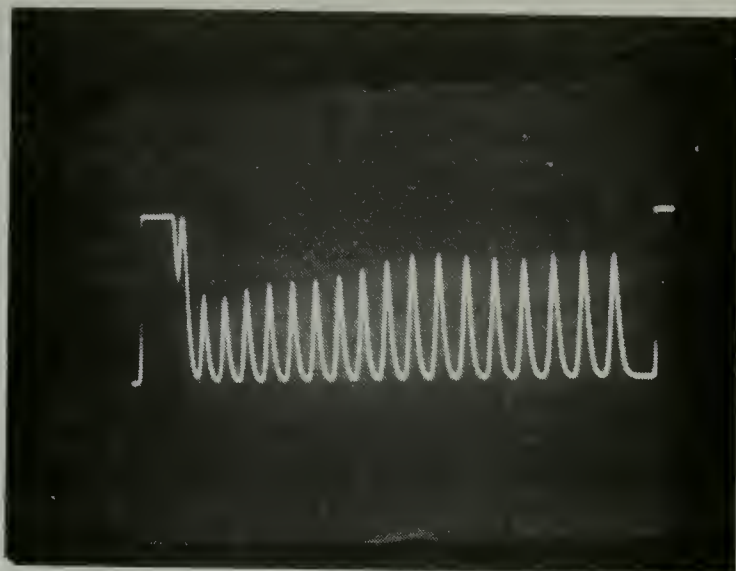


FIGURE 28. Beat frequency (uncorrected) as recorded at input to PLL

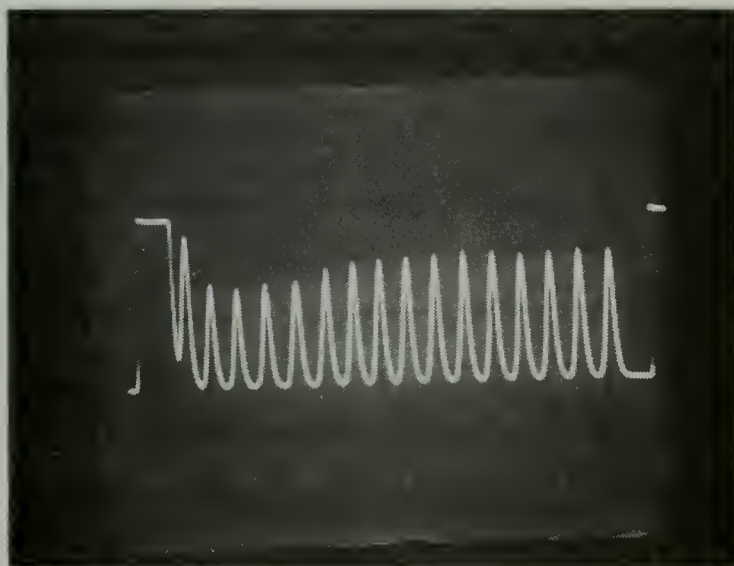


FIGURE 29. Beat frequency (corrected) as recorded at input to PLL



$$\left(\frac{df}{dt}\right) = \frac{f_B}{\Delta t}$$

$$\Delta\left(\frac{df}{dt}\right) = \frac{\Delta f_B}{\Delta t} \quad \text{where } \Delta f_B = (\text{beat frequency measured} \\ - 187 \text{ KHz})$$

$$\frac{\Delta\left(\frac{df}{dt}\right)}{\left(\frac{df}{dt}\right)} = \frac{\Delta f_B (100\%)}{f_B}$$

The above expression gives the percentage deviation from linearity for the output-frequency slope.

The beat frequency was monitored as outlined in the beat-frequency method of Section VI. The time between each successive peak of the beat frequency was measured and converted to a corresponding frequency. The difference between these frequencies and 187 KHz was recorded. Three sets of data are plotted in Figure 30 showing percentage deviation from linearity of the output-frequency slope versus time. Each of these represents a slightly different bias on the varactor. On the same figure is also plotted the uncorrected deviation.

In analyzing the corrected curves of Figure 30, the deviation oscillated around the desirable. The worst case deviation above was approximately 7% while the worst case deviation below was approximately 9%. However, the uncorrected curve deviated above by 14% and below by 18%. Thus, indications are that linearity errors have been reduced by approximately 50% for the worst case deviations.





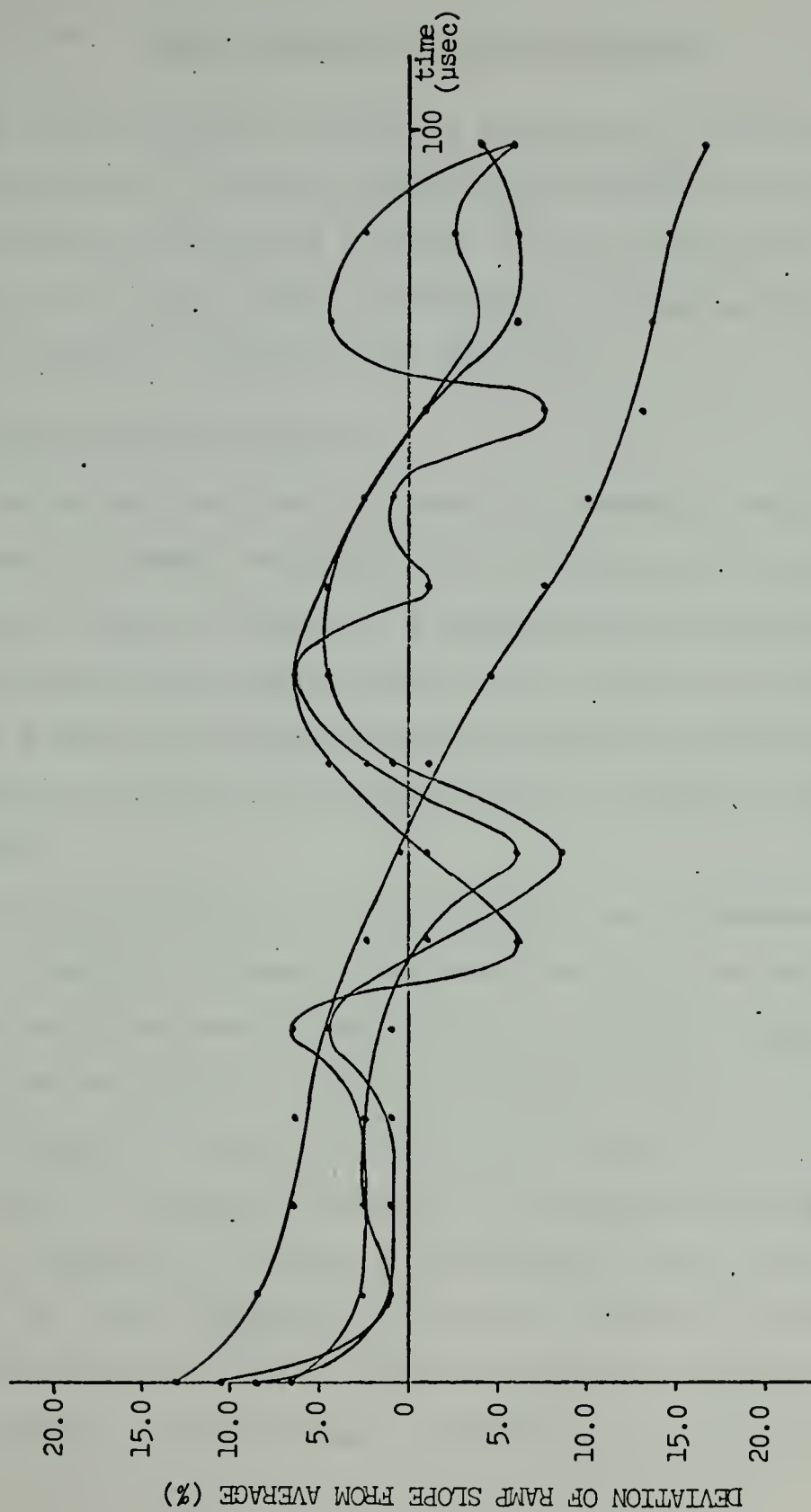


FIGURE 30. Deviation of ramp slope,  $df/dt$ , from average



#### XIV. OTHER METHODS OF FM LINEARIZATION

Two other methods capable of linearizing the FM sweep were postulated, but time limitations prohibited the actual construction and testing of each. The following few paragraphs will offer a brief description of these methods and their ability to linearize the FM sweep.

##### A. SAMPLE-AND-HOLD METHOD

This method utilizes a linear discriminator which produces a voltage proportional to the period of the beat-frequency signal by means of a sample-and-hold circuit, a ramp generator and gating pulses. The process is simply to sample a gated ramp signal once each cycle of the beat frequency and apply the sampled value of voltage on the varactor.

The ramp generator is in the form of an integrator with a constant voltage on the input and is to be gated on as the beat frequency starts a cycle. The ramp signal is placed on the input to a sample-and-hold circuit. Prior to reinitiating the ramp generator at the beginning of the next cycle of the beat frequency, the sample-and-hold circuit should be gated on in order to sample the ramp at the input.

If the beat frequency is high, the ramp will not reach a high value because the period of the beat frequency for that cycle is short and ramp reinitiation will occur in a



shorter time. Conversely, if the beat frequency is low, the ramp has a larger time before reinitiation and will reach a higher value.

From the above, it is seen that the higher the beat frequency, the lower the signal from the sample-and-hold circuit. The reference point for the output from the sample-and-hold circuit may be chosen as that value produced by the desired beat frequency component. Then, portions of the beat frequency signal where frequency is above that desired will cause a decrease while those below that desired will cause an increase in the voltage levels placed on the varactor. The net result is a linearizing of the output-frequency waveform.

Two possible methods of implementing the sample and hold technique are outlined in Figures 31, 32 and 33, and Figures 34 and 35.

#### B. ANALOG/DIGITAL METHOD

All methods discussed so far for linearizing the FM sweep have utilized analog means. The following discussion outlines a method for achieving the same results with a large portion of the correcting circuit being digital. In the following method the voltage ramp placed on the varactor would be generated digitally with subsequent error signals added to it in a digital adder.



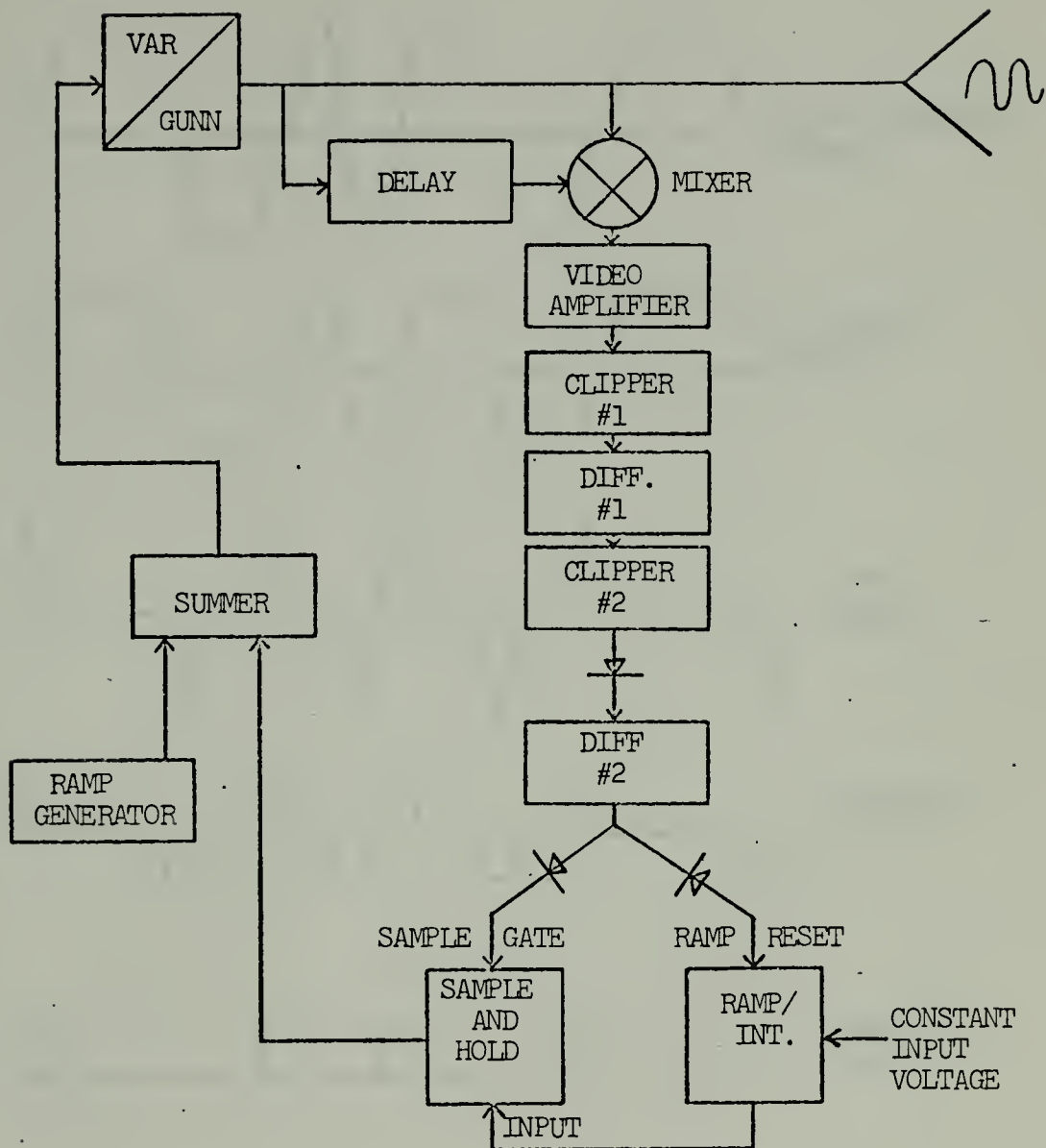


FIGURE 31. Sample and hold method no. 1 block diagram





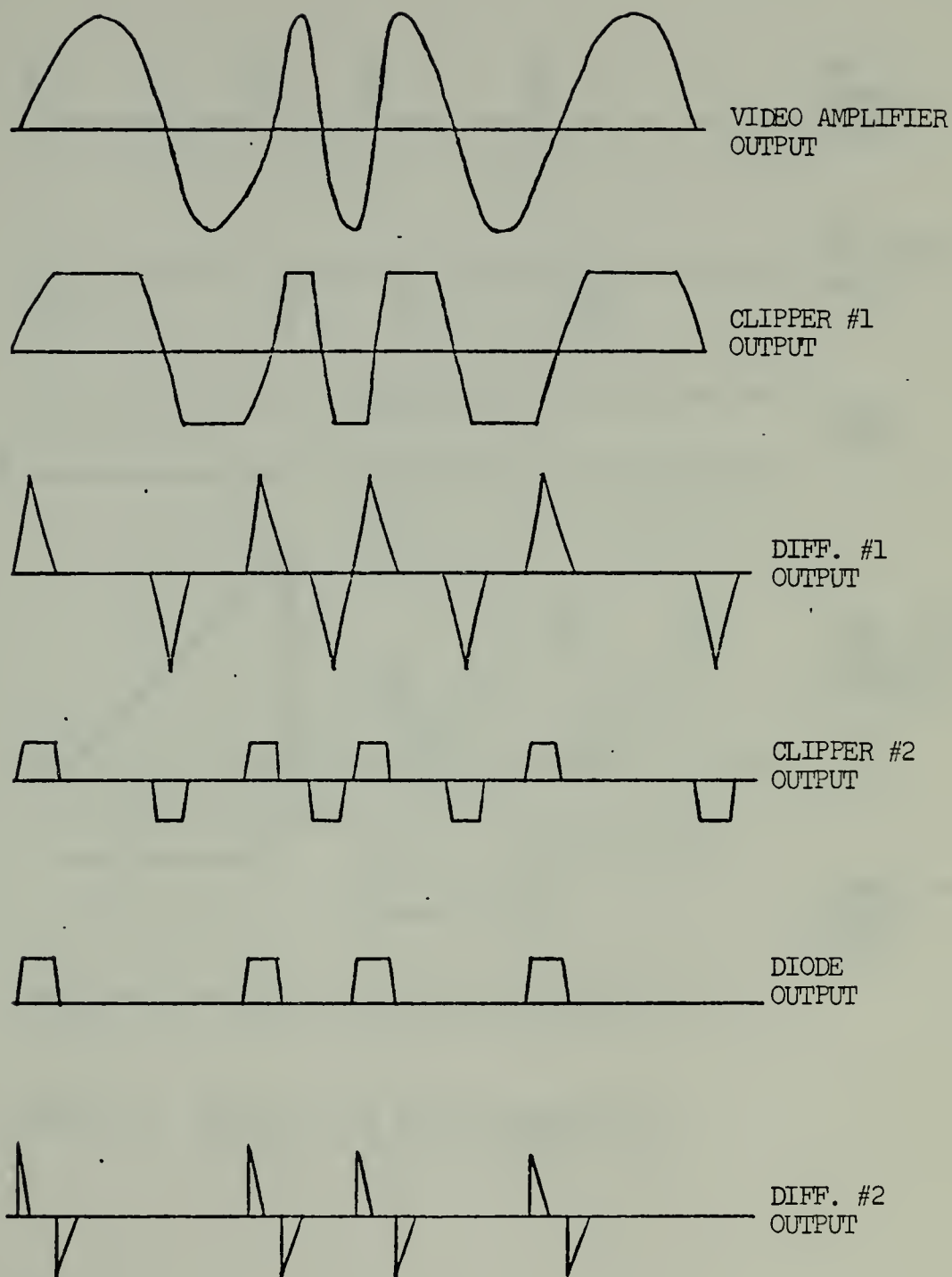


FIGURE 32. Sample and hold method no. 1  
circuit waveforms (Part I)



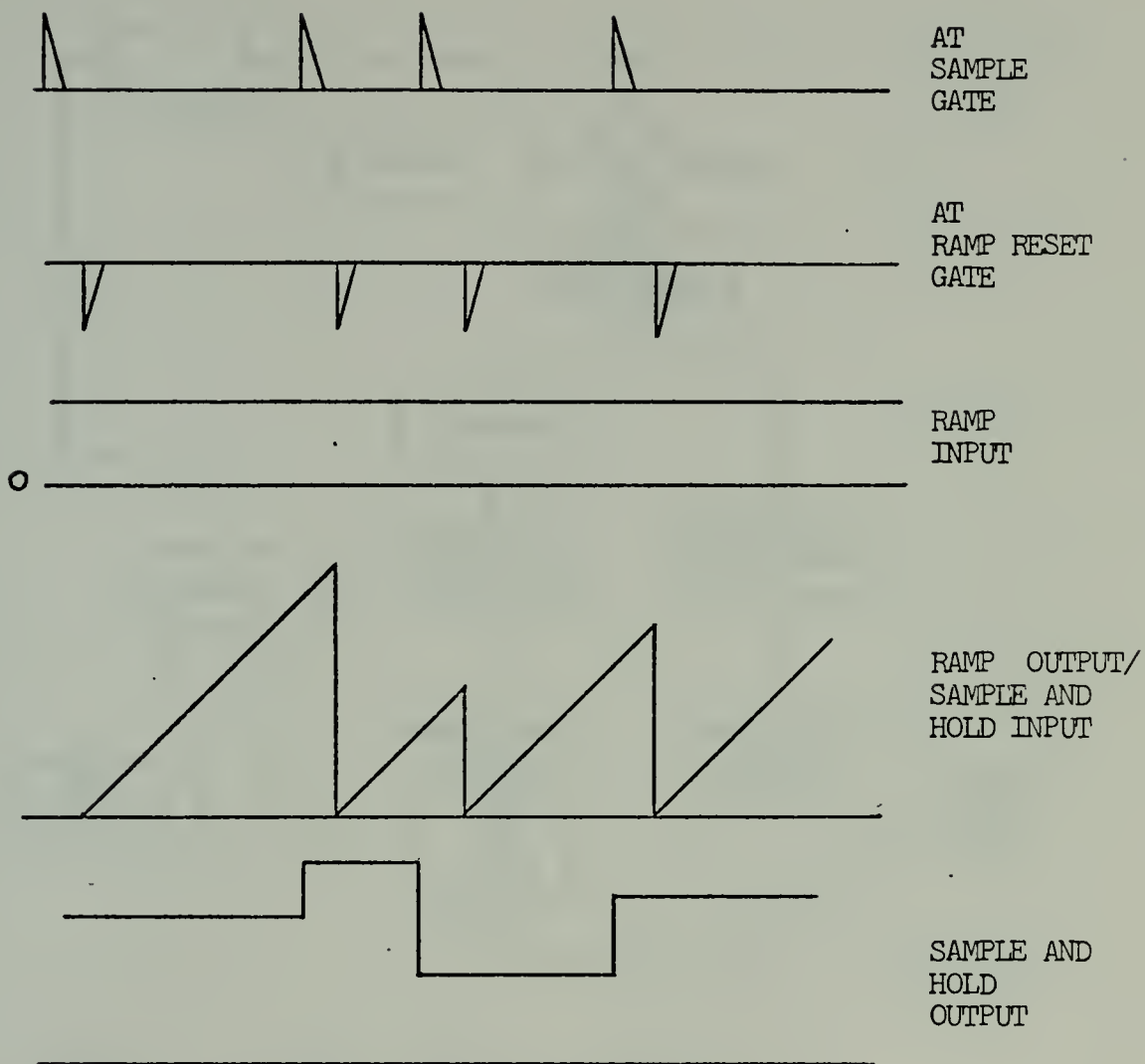


FIGURE 33. Sample and hold method no. 1 circuit waveforms (Part II)



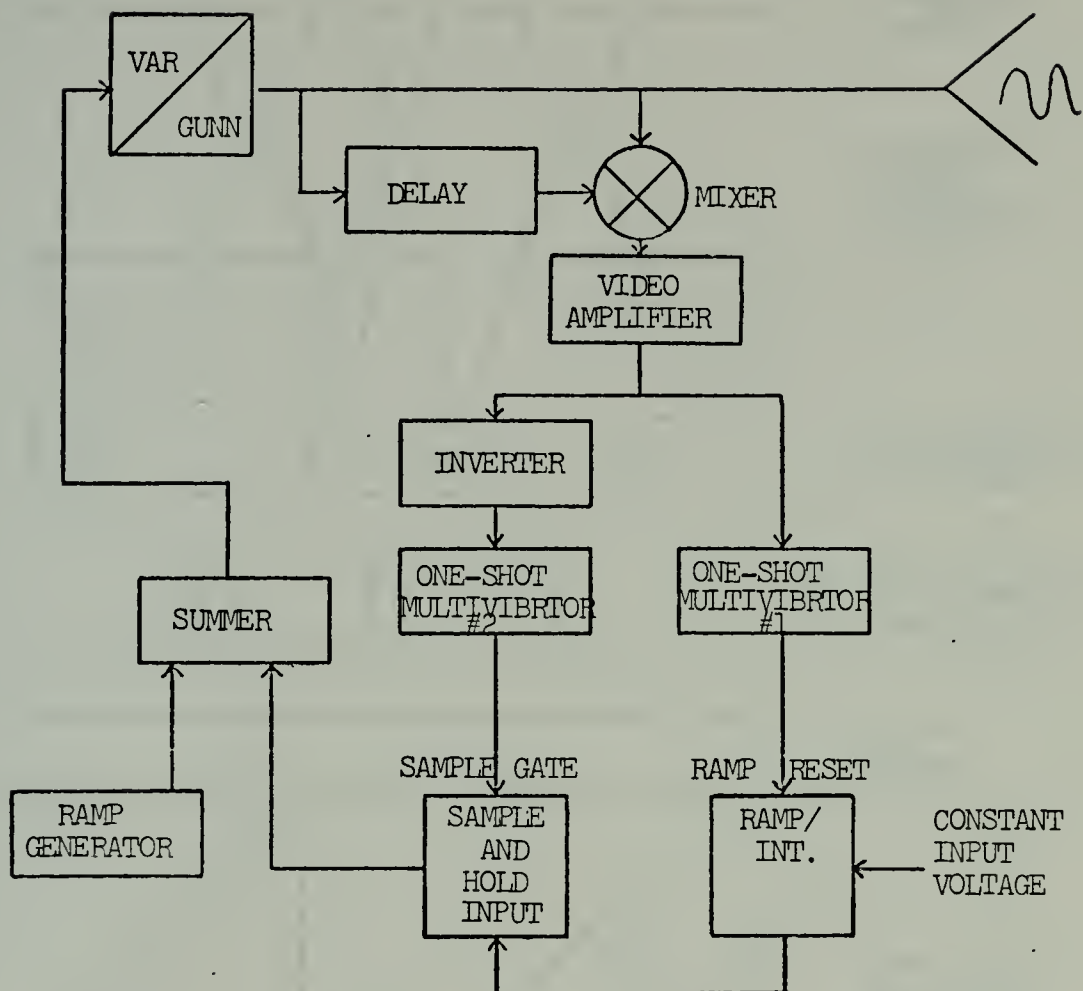


FIGURE 34. Sample and hold method no. 2 block diagram



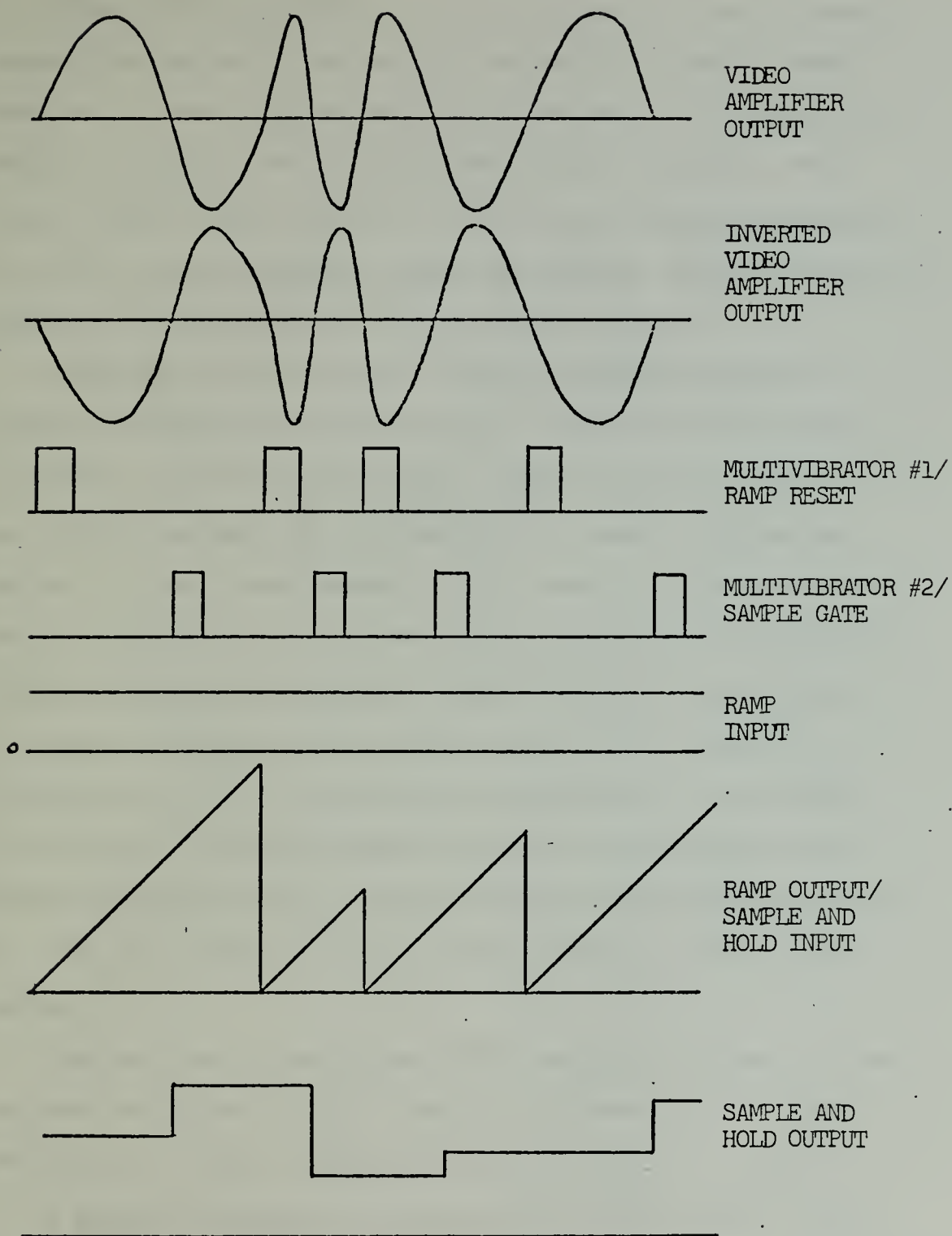


FIGURE 35. Sample and hold method no. 2 circuit waveforms





Figure 36 illustrates a block diagram of the proposed correcting method. The major components include a ramp counter, a bank of parallel shift registers, a digital-to-analog converter, two digital adders and a clock. The input marked "error signal" on the block diagram represents an error signal from the system in digital form. A possible method for achieving this is discussed later.

The ramp is generated by simply clocking the ramp counter through its entire range. The clock must be set at such a rate that the counter reaches maximum count in the time necessary for one modulation sweep (modulation period) of the radar system. For example, if the counter was an 8-bit device, it must be clocked from 0 through 256 counts during one modulation period. If the period were 100  $\mu$ sec, then the clock must count to 256 in 100  $\mu$ sec or 256 counts per 100  $\mu$ sec which corresponds to a 2.56 MHz clock rate. Thus the number of bits in the ramp counter establishes how small each step in the ramp staircase will be, and the clock rate sets up the timing for the whole system.

The required size of the shift register depends on the maximum deviation of the slope from linearity. If this deviation is small, the shift register could be small.

A possible method for generation of the digital error signal is shown in block diagram form in Figure 37. The idea uses the method described in this thesis for generating an analog error signal out of the phase-locked loop. From the



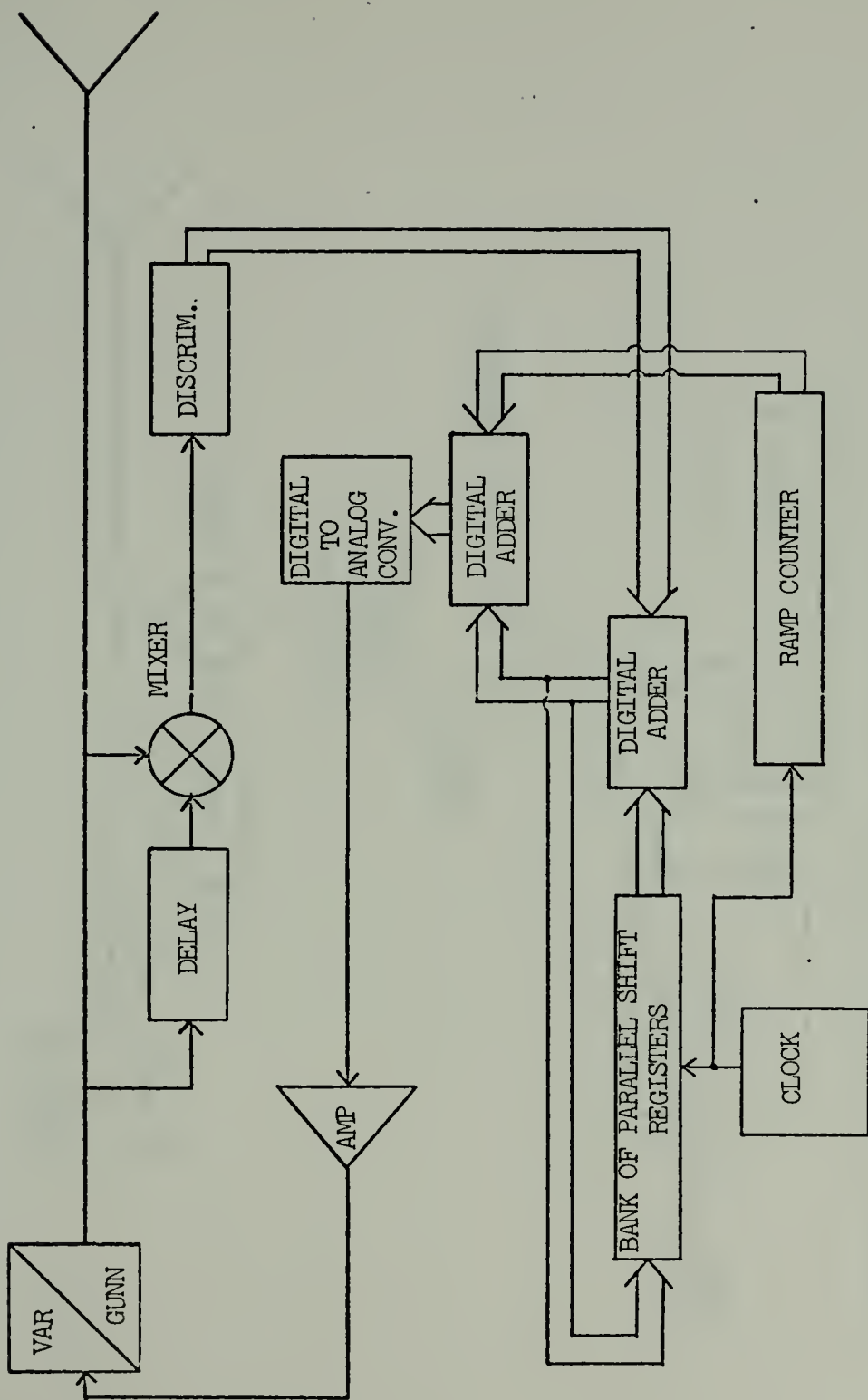


FIGURE 36. Block diagram of analog/digital linearizing method



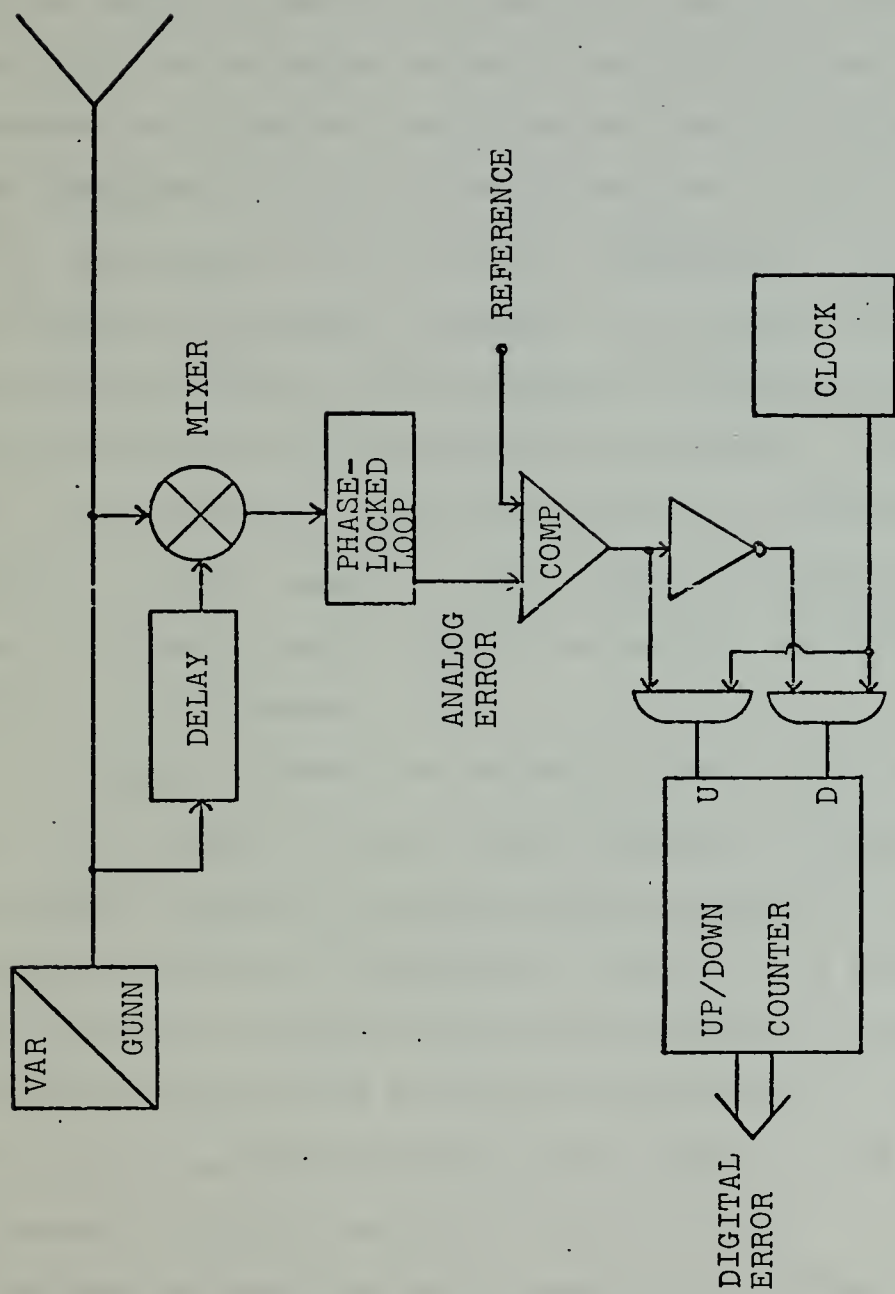


FIGURE 37. Analog to digital error conversion



output of the PLL, the analog error would be compared to a reference value established for the zero-error state. The output from the comparator through steering gates causes an up/down counter to be clocked either up or down. The resulting output from the counter is a digital signal proportional to the error sensed. The clock in this arrangement could be the same clock as used in Figure 36.

An advantage of this method is that the total signal sent to the varactor is not only a combination of the present error signal and the ramp voltage, but it also includes the error which was sent to the varactor at precisely the same correcting instant one modulation cycle before. In this manner, the correcting system should reach a steady-state such that the error signal to the varactor is based primarily on past information with a resulting minimum deviation from linearity in the system.

In a certain manner, the correcting system is predicting what the error should be at a given instant from past information, comparing the predicted error with the actual instantaneous error of the system to arrive at a new error signal, summing this error signal with the ramp for application on the varactor and storing this same value of error signal for use as the predicted error signal at the same time instant the next modulation cycle.

The ramp retrace time would probably be limited by the settling time of the D/A converter which should be less than





1.0  $\mu$ sec. With retrace time this short, the low end correction problems as discussed in Section XI and receiver/transmitter blanking time would be reduced.



## XV. CONCLUSION

Varactor-tuned Gunn oscillators have operating characteristics which make them desirable for application as RF sources in portable marine FM-CW radars. When the Gunn device is used in this application, it is very important that the output-frequency sweep vary linearly with time. Any deviation from linearity throughout the output-frequency sweep, will cause a loss of range resolution in the system. The output-frequency sweep of the typical varactor-tuned Gunn oscillator is inherently non-linear, with the degree of non-linearity increasing with increasing sweep widths. Therefore, in order to achieve frequency-modulation linearity while using large sweep widths, it becomes necessary to linearize the frequency sweep. One method of linearizing the sweep was developed in detail, while several others were outlined, in this thesis. The approach to linearization used in this thesis was successful, but it was limited by both the inability of the system to correct errors instantly and the lack of quality correcting during the ramp retrace. Better results would have been possible if the retrace time had been shorter and the beat frequency had been longer. The method requiring digital generation of the ramp and error signal or some variation of it, is predicted to be the most effective means for linearizing the frequency sweep.



## LIST OF REFERENCES

1. Luck, D.G.C., Frequency Modulated Radar, p. 3, McGraw-Hill, 1949.
2. Sobol, H. and Sterzer, F., "Microwave Power Sources," I.E.E.E. Spectrum, p. 29, April 1972.
3. Bushnell, T.R., and Isaacs, A.T., "Wideband Varactor-Tuned Solid-State Sources to 20 GHz," The Microwave Journal, p. 45-48, June 1973.
4. Times Wire and Cable Company, RF Transmission Line Catalog and Handbook, No. TL3, 1970.
5. Luck, D.G.C., Frequency Modulated Radar, p. 7, McGraw-Hill, 1949.
6. Skolnik, M.I., Introduction to Radar Systems, p. 72, McGraw-Hill, 1962.
7. Luck, D.G.C., Frequency Modulated Radar, p. 27-28, McGraw-Hill, 1949.
8. Rodrigue, G.P., "Microwave Solid-State Delay Lines," Proceedings of the I.E.E.E., Volume 53, No. 10, p. 1428-1437, October 1965.
9. Hymans, A.J., and Lait, J., "Analysis of a Frequency-Modulated Continuous Wave Ranging System," I.E.E. Paper No. 3264E, July 1960.
10. Ginzton, E.L., Microwave Measurements, p. 405-407, McGraw-Hill, 1957.
11. Millman, J. and Taub, H., Pulse, Digital, and Switching Waveforms, p. 514-569, McGraw-Hill, 1965.
12. Signetics Corporation, Applications Handbook, p. 6-1, 1974.
13. Signetics Corporation, Applications Handbook, p. 6-6, 1974.



INITIAL DISTRIBUTION LIST

	No. Copies
1. Defense Documentation Center Cameron Station Alexandria, Virginia 22314	2
2. Library, Code 0212 Naval Postgraduate School Monterey, California 93940	2
3. Professor David B. Hoisington, Code 52 Hs Department of Electrical Engineering Naval Postgraduate School Monterey, California 93940	1
4. Teledyne MEC 3165 Porter Drive Palo Alto, California 94394 ATTN: Mr. Ernie Kirchner	1
5. LT. Steven A. Marshall, USN 1133 Burke Drive Gallup, New Mexico 97301	1









Thesis

158397

M3559 Marshall

c.1 Linearization of  
FM-CW radar sweep by  
feedback.

Thesis

158397

M3559 Marshall

c.1 Linearization of  
FM-CW radar sweep by  
feedback.

thesM3559

Linearization of FM-CW radar sweep by fe



3 2768 001 03431 7

DUDLEY KNOX LIBRARY